DNA-TR-88-142

AD-A213 754

TARGET AREA OPERATING CONDITIONS

Saharan Dust Plumes as an Analogue for Nuclear Dust Clouds

R. A. Gaj
R. D. Small
Pacific-Sierra Research Corporation
12340 Santa Monica Boulevard
Los Angeles, CA 90025-2587

10 June 1988

Technical Report

CONTRACT No. DNA 001-87-C-0298

Approved for public release;
distribution is unlimited.

THIS WORK WAS SPONSORED BY THE DEFENSE NUCLEAR AGENCY UNDER RDT&E RMC CODES B4662D RA RG 001223420 25904D AND B4662D RA RG 101224400 25904D.

Prepared for
Director
Defense Nuclear Agency
Washington, DC 20305-1000

Destroy this report when it is no longer needed. Do not return to sender.

PLEASE NOTIFY THE DEFENSE NUCLEAR AGENCY, ATTN: CSTI, WASHINGTON, DC 20305-1000, IF YOUR ADDRESS IS INCORRECT, IF YOU WISH IT DELETED FROM THE DISTRIBUTION LIST, OR IF THE ADDRESSEE IS NO LONGER EMPLOYED BY YOUR ORGANIZATION.

Director
Defense Nuclear Agency
ATTN: TITL
Washington, DC 20305-1000

Director
Defense Nuclear Agency
ATTN: TITL
Washington, DC 20305-1000

DISTRIBUTION LIST UPDATE

This mailer is provided to enable DNA to maintain current distribution lists for reports. We would appreciate your providing the requested information.

- ☐ Add the individual listed to your distribution list.
- ☐ Delete the cited organization/individual.
- ☐ Change of address.

NAME: _____

ORGANIZATION: _____

OLD ADDRESS	CURRENT ADDRESS
_____	_____
_____	_____
_____	_____

TELEPHONE NUMBER: ( ) _____

SUBJECT AREA(s) OF INTEREST:

_____	_____
_____	_____
_____	_____

DNA OR OTHER GOVERNMENT CONTRACT NUMBER: _____

CERTIFICATION OF NEED-TO-KNOW BY GOVERNMENT SPONSOR (if other than DNA):

SPONSORING ORGANIZATION: _____

CONTRACTING OFFICER OR REPRESENTATIVE: _____

SIGNATURE: _____

CUT HERE AND RETURN

REPORT DOCUMENTATION PAGE

1a REPORT SECURITY CLASSIFICATION UNCLASSIFIED	1b RESTRICTIVE MARKINGS
2a SECURITY CLASSIFICATION AUTHORITY N/A since Unclassified	3 DISTRIBUTION/AVAILABILITY OF REPORT Approved for public release; distribution is unlimited
2b DECLASSIFICATION/DOWNGRADING SCHEDULE N/A since Unclassified	
4 PERFORMING ORGANIZATION REPORT NUMBER(S) PSR Report 1817	5 MONITORING ORGANIZATION REPORT NUMBER(S) DNA-TR-88-142
6a NAME OF PERFORMING ORGANIZATION Pacific-Sierra Research Corporation 6b OFFICE SYMBOL (if applicable)	7a NAME OF MONITORING ORGANIZATION Director Defense Nuclear Agency
6c ADDRESS (City, State, and ZIP Code) 12340 Santa Monica Boulevard Los Angeles, CA 90025-2587	7b ADDRESS (City, State, and ZIP Code) Washington, DC 20305-1000
8a NAME OF FUNDING/SPONSORING ORGANIZATION 8b OFFICE SYMBOL (if applicable) SPWE/Galloway	9 PROCUREMENT INSTRUMENT IDENTIFICATION NUMBER DNA 001-87-C-0298
8c ADDRESS (City, State, and ZIP Code)	10 SOURCE OF FUNDING NUMBERS

PROGRAM ELEMENT NO.	PROJECT NO.	TASK NO.	WORK UNIT ACCESSION NO
62715H	RA	RG	DH702980

11 TITLE (Include Security Classification)
TARGET AREA OPERATING CONDITIONS
Saharan Dust Plumes as an Analogue for Nuclear Dust Clouds

12 PERSONAL AUTHOR(S)
Gaj, R. A.; Small, R. D.

13a TYPE OF REPORT	13b TIME COVERED	14 DATE OF REPORT (Year, Month, Day)	15 PAGE COUNT
Technical	FROM 870929 TO 880610	880610	38

16 SUPPLEMENTARY NOTATION
This work was sponsored by the Defense Nuclear Agency under RDT&E RMC Codes B4662D RA RG 001223420 25904D and B4662D RA RG 101224400 25904D.

17 COSATI CODES			18 SUBJECT TERMS (Continue on reverse if necessary and identify by block number)		
FIELD	GROUP	SUB-GROUP	Dust	Saharan Plumes	Dust Transport
18	3		Optical Depth	Scouring	Dust Cloud Depletion
15	6		Particle-Size Distribution	Nuclear Bursts	

19 ABSTRACT (Continue on reverse if necessary and identify by block number)

Saharan dust plumes are examined as natural analogues for nuclear dust clouds. Lofting mechanisms, dust injection altitudes, particle-size distributions, long-range transport processes, removal mechanisms, depletion rates, and radiative effects are discussed and compared. ~~We find that~~ Saharan dust storms can loft masses comparable to about one-third the injection expected from a counterforce attack against a U.S. missile silo field; the exact amount depends on soil type and condition, vegetation, and season. A Saharan plume extends several thousand kilometers downstream and is usually confined below 4 to 6 km altitude. The long-range transport is aided by (1) the presence of a stable layer in the lower troposphere and (2) the lack of precipitation scavenging. Nuclear dust clouds, which would encounter mid-latitude precipitation systems, would be more rapidly depleted in the lower troposphere. ~~We demonstrate~~ that this depletion is sensitive to the initial concentration of submicron-size particles

20 DISTRIBUTION/AVAILABILITY OF ABSTRACT	21 ABSTRACT SECURITY CLASSIFICATION	
☐ UNCLASSIFIED/UNLIMITED ■ SAME AS RPT ☐ DTIC USERS	UNCLASSIFIED	
22a NAME OF RESPONSIBLE INDIVIDUAL Bennie F. Maddox	22b TELEPHONE (Include Area Code) (202) 325-7042	22c OFFICE SYMBOL DNA/CSTI

DD Form 1473, JUN 86 *Previous editions are obsolete.*

19. ABSTRACT (Continued)

in the stabilized nuclear cloud. ~~We find that~~ the Saharan dust plume provides an appropriate analogue for dust removal from the lower troposphere in the absence of precipitation.

PREFACE

This report summarizes Pacific-Sierra Research Corporation's study of obscurations and turbulence created by dust, smoke, and fires in target areas after a nuclear laydown. The work, presented in two volumes, was performed under contract DNA 001-87-C-0298. The technical adviser for this work was Dr. C. Galloway.

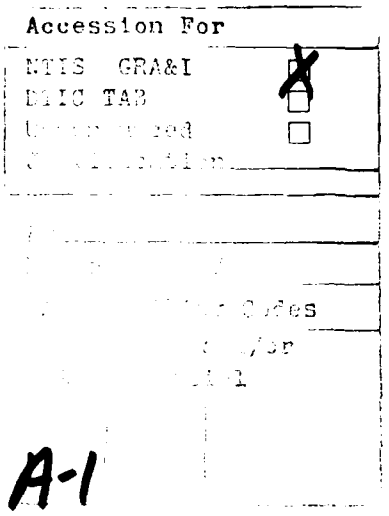

CONVERSION TABLE

Conversion factors for U.S. customary
to metric (SI) units of measurement

To Convert From	To	Multiply By
angstrom	meters (m)	1 000 000 X E-10
atmosphere	kilo pascal (kPa)	1.013 25 X E + 2
bar	kilo pascal (kPa)	1.000 000 X E + 2
barn	meter^2 (m^2)	1.000 000 X E-28
British Thermal unit (thermochemical)	joule (J)	1.054 350 X E + 3
calorie (thermochemical)	joule (J)	4.184 000
cal (thermochemical)/cm^2	mega joule/m2(MJ/m2)	4 184 000 X E-2
curie	giga becquerel (GBq)*	3.700 000 X E + 1
degree (angle)	radian (rad)	1.745 329 X E-2
degree Fahrenheit	degree kelvin (K)	$T_K=(t°f + 459.67)/1$ 8
electron volt	joule (J)	1.602 19 X E-19
erg	joule (J)	1.000 000 X E-7
erg/second	watt (W)	1.000 000 X E-7
foot	meter (m)	3.048 000 X E-1
foot-pound-force	joule (J)	1.355 818
gallon (U.S. liquid)	meter^3 (m^3)	3.785 412 X E-3
inch	meter (m)	2.540 000 X E-2
jerk	joule (J)	1.000 000 X E + 9
joule/kilogram (J/Kg) (radiation dose absorbed)	Gray (Gy)**	1.000 000
kilotons	*terajoules*	4.183
kip (1000 lbf)	newton (N)	4.448 222 X E + 3
kip/inch^2 (ksi)	kilo pascal (kPa)	6.894 757 X E + 3
ktap	newton-second/m^2 (N-s/m^2)	1.000 000 X E + 2
micron	meter (m)	1.000 000 X E-6
mil	meter (m)	2.540 000 X E-5
mile (international)	meter (m)	1.609 344 X E + 3
ounce	kilogram (kg)	2.834 952 X E-2
pound-force (lbf a voirdupois)	newton (N)	4.448 222
pound-force inch	newton-Ometer (N.m)	1.129 848 X E-1
pound-force/inch	newton/meter (N/m)	1.751 268 X E + 2
pound-force/foot^2	kilo pascal (kPa)	4.788 026 X E-2
pound-force/inch^2	kilo pascal (kPa)	6.894 757
pound-mass (ibm a voirdupois)	kilogram (kg)	4.535 924 X E-1
pound-mass-foot^2 (moment of inertial)	kilogram-meter2 (kg.m^2)	4.214 011 X E-2
pound-mass/foot^3	kilogram/meter3 (kg/m^3)	1.601 846 X E + 1
rad (radiation dose absorbed)	Gray (Gy)**	1.000 000 X E-2
roentgen	coulomb/kilogram (C/kg)	2.579 760 X E-4
shake	second (s)	1.000 000 X E-8
slug	kilogram (kg)	1.459 390 X E + 1
torr (mm Hg. 0°C)	kilo pascal (kPa)	1.333 22 X E-1

*The becquerel (Bq is the SI unit of radioactivity: Bp = 1 event/s.

**The Gray (Gy) is the SI unit of absorbed radiation.

TABLE OF CONTENTS

Section		Page
	PREFACE	iii
	CONVERSION TABLE	iv
	FIGURES	v
1	INTRODUCTION	1
2	SAHARAN DUST PLUMES	2
	SOURCE STRENGTH	2
	DISTRIBUTION PATTERNS	2
	SEASONAL DIFFERENCES	2
	PLUME DEVELOPMENT	2
	SAHARAN AIR LAYER	5
	MASS DEPLETION RATES	8
	PARTICLE-SIZE DISTRIBUTION	8
	REMOVAL MECHANISMS	12
	RADIATIVE EFFECTS	14
3	LOFTING MECHANISMS	17
	VERTICAL MASS FLUX	17
	THRESHOLD VELOCITY	17
4	NUCLEAR DUST ANALOGUE	20
	LOFTING MECHANISMS	20
	LONG-RANGE TRANSPORT	20
	DEPLETION RATES	20
	RADIATIVE EFFECTS	25
5	CONCLUSIONS	27
6	LIST OF REFERENCES	28

FIGURES

Figures		Page
1	Saharan dust distribution patterns and estimated mass fluxes (in teragrams per year)	3
2	Average Saharan plume positions and mean 700 mbar (≈ 3 km) streamline fields for winter and summer (Location of Sahara indicated by hatching.)	4
3	Schematic of major processes involved in lofting, transport, and removal of Saharan dust from atmosphere.	6
4	Typical summer temperature profile over tropical north Atlantic near African coast.	7
5	Normalized column density in Saharan plume as function of distance down stream.	9
6	Mass depletion rate in Saharan plume as function of distance down-stream	10
7	Representative particle-size distributions in Saharan plume.	11
8	Effect of various dust removal mechanisms on Saharan dust particle-size distribution after 48-h simulation time.	13
9	Observed dust optical depths (λ = 0.66 μm) in Saharan plume for 0942 GMT, 30 July 1974.	15
10	Dependence of vertical dust mass flux from surface on friction velocity.	18
11	Comparison of simulated vertical dust concentration profiles in Saharan plume and nuclear dust cloud.	21
12	Three hypothetical power-law PSDs for low-altitude nuclear bursts and least-squares fit to observed subsurface burst PSD (mass concentration is 700 $\mu g/m^3$).	24
13	Computed normalized column densities as function of distance downstream for four initial PSDs.	26

SECTION 1

INTRODUCTION

Nuclear explosions at or near the surface of the earth inject large quantities of dust and debris high into the atmosphere. The net injection in a full-scale nuclear exchange is estimated to be as much as several hundred teragrams [Turco et al., 1983; National Research Council (NRC), 1985; Pittock et al., 1986; Bacon, Dunn, and Sarma, 1988]. The presence of so much dust in the atmosphere could have many serious consequences, ranging from interference with military operations to changes in the global climate. Simple models have been developed to help assess the impact of nuclear dust. Yet, because our knowledge of the lofting, transport, removal, and optical effects of large atmospheric dust masses is limited, these models rely on several assumptions that are highly uncertain.

Opportunities to experimentally study the physics of nuclear dust clouds ended with above ground testing in 1962. Available data are either insufficient or not completely analyzed. One alternative is to identify natural events that display some of the key physical mechanisms believed to be important in nuclear dust clouds. Two natural analogues are promising: (1) plumes from erupting volcanos and (2) Saharan dust storms. Volcanic plumes have been considered an analogue for high altitude dust transport [see, for example, NRC, 1985]. Such plumes may also model condensation processes (for crater ejecta) that occur at upper altitudes. In this report, we examine Saharan dust plumes, and evaluate their relevance as an analogue for nuclear dust clouds.

The most attractive feature of Saharan plumes is the amount of dust involved. A single storm usually lasts about four or five days, and typically transports 8 to 10 Tg of dust westward from the Sahara over the Atlantic Ocean [Carlson, 1979]. Assuming a dust lofting capacity for nuclear surface bursts of 0.3 Tg/MT [Rosenblatt, 1981], a Saharan dust episode equals roughly thirty 1-MT surface detonations or about one-fifth the injection expected from a full-scale (counterforce) attack against a single U.S. Minuteman missile field[1] [Bacon, Dunn, and Sarma, 1988].

Since Saharan plumes contain such a large quantity of lofted material, they are easily monitored by satellites. Over the ocean, the highly reflective plume contrasts well against the water. Moreover, aerosol particles of true Saharan origin (which are usually composed of quartz grains and clay) and locally generated aerosols (i.e., sea salt particles) are readily distinguished at sampling stations far from the source. Thus, key aspects of the dust plume such as its density and its particle-size distribution (PSD) can be measured as a function of downstream distance. To the extent that a Saharan plume resembles a nuclear dust cloud, we can learn about (1) the possible optical and climate effects of nuclear dust, (2) radioactive fallout patterns, (3) erosive and mechanical hazards dust presents to aircraft, and (4) sedimentation rates.

In Sec. 2, we review meteorological and geographical aspects, long-range transport and removal mechanisms, and optical effects. The physical mechanisms involved in the lofting of wind-blown dust are discussed in Sec. 3. Saharan dust plumes as analogues for nuclear dust clouds are evaluated in Sec. 4, and our conclusions are summarized in Sec. 5.

1. Assuming 165 targets per field and a scenario involving one 500-KT surface burst and one 500-KT low-altitude airburst per target.

SECTION 2

SAHARAN DUST PLUMES

SOURCE STRENGTH.

The Sahara is the single largest source of wind-blown atmospheric dust in the world. It is estimated that the Sahara generates from 130 to 330 Tg per year [Prospero and Carlson, 1972; Jaenicke and Sch 1978; Ganor and Mamane, 1982]. This is roughly one-quarter to one-half of the total annual dust generated by all sources worldwide, and accounts for about the same fraction of the total dust burden found in the atmosphere at any given time [Junge, 1979]. The Sahara probably contributes almost as much mass to the global dust budget as all other major sources combined (e.g., the Rajashan Desert of India, the Gobi Desert of Mongolia and northern China, and the deserts of Mexico and the southwestern U.S.). The Saharan dust mass is usually added to the atmosphere in 10 to 12 storms per year, ranging in size from 0.1 to 10Tg. The largest storms raise a mass comparable to surface bursts yielding tens of megaton. The source region for Saharan dust storms can cover several thousand square kilometers, roughly equivalent to a section of a missile field.

DISTRIBUTION PATTERNS.

We are concerned primarily with the westward transport of dust from the Sahara to the Atlantic Ocean. Significant amounts are also carried in other directions. Figure 1 shows a composite of several dust transport estimates. Although most of the lofted mass is carried westward, approximately 20 percent (70 Tg/year) is transported eastward toward the eastern Mediterranean. Lesser amounts (in unknown quantities) are also carried north and south, as evidenced by occasional dust falls over Europe [Tullet, 1978; Prodi and Fea, 1979] and the Gulf of Guinea [Bertrand, Baudet, and Drochon, 1974].

Most of the dust raised from the Sahara consists initially of particles with radii greater than 1 μm. These particles have high fall velocities and therefore do not remain lofted for very long. Figure 1 shows the magnitude of this prompt depletion: Of the approximately 330 Tg/year raised over the Sahara, only about one-quarter (90 Tg/year) eventually leaves the African continent. Of the remainder, about 40 percent (135 Tg/year) is deposited in the Atlantic Ocean, another 40 percent crosses the Atlantic, and 20 percent falls over the Near East. Although a significant fraction remains in the atmosphere and is transported several thousand kilometers by wind systems, most particles fall out in the first 500 to 1000 km from the source. The depletion—mostly in micron or larger sized particles—is similar to that anticipated in nuclear clouds.

SEASONAL DIFFERENCES.

Westward dust transport from the Sahara is perennial, but seasonal differences in the distribution occur (caused by changes in major wind patterns across Africa). Figure 2 shows the average summer and winter locations of the Saharan plume from satellite observations [Schütz, 1980]. The mean streamlines at the effective steering altitude (about 3 km) are also shown. In winter (Fig. 2a), direct transport from the Sahara to the Atlantic is blocked by the mean westerlies over north Africa. The plume therefore emerges somewhat below the Sahara over the Gulf of Guinea and extends southwestward toward Brazil with the mean easterlies. In summer (Fig. 2b), these easterlies shift northward and direct transport from the Sahara resumes. The summer dust is then carried almost due west. This seasonal shift is therefore responsible for the sharp summer maximum (and winter minimum) in dust concentrations noted at Barbados Island [Carlson and Prospero, 1972].

Although these seasonal differences are mostly due to changes in weather patterns, there are also seasonal differences in dust cloud composition [Delany et al., 1967; Prospero et al., 1970]. In summer (the rainy season in sub-Saharan Africa), grasses inhibit dust scouring. Similarly, rainfall changes the soil cohesiveness. Consequently, the seasonal dependence is strong. A similar, but more pronounced dependence is expected for U.S. and Soviet target areas, especially in regions where soil freezing occurs.

PLUME DEVELOPMENT.

The large summertime Saharan dust loads are caused by: (1) the presence of a strong, per-

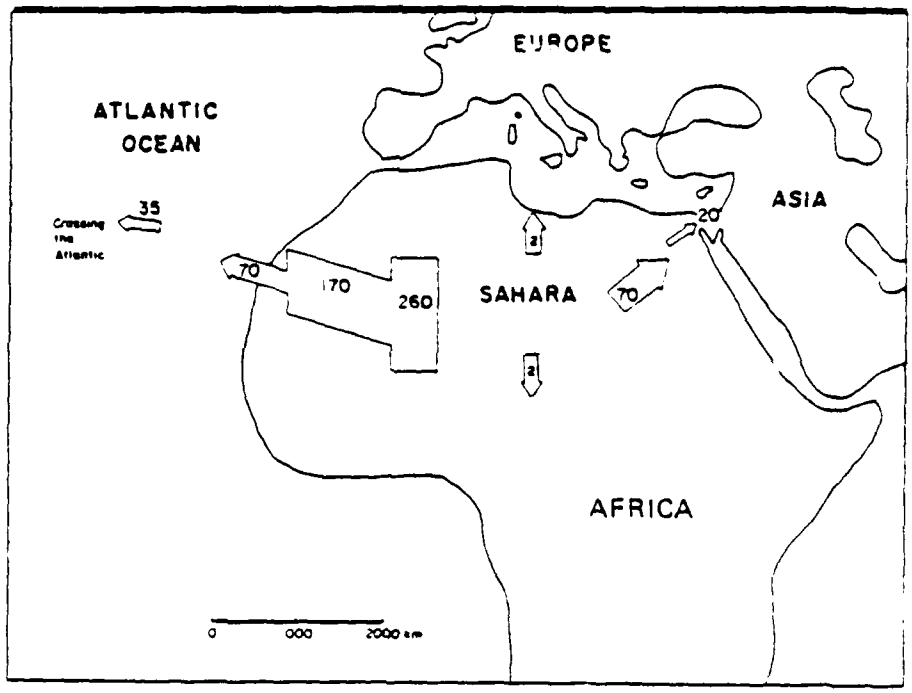

Figure 1. Saharan dust distribution patterns and estimated mass fluxes (in teragrams per year)

a. Winter.

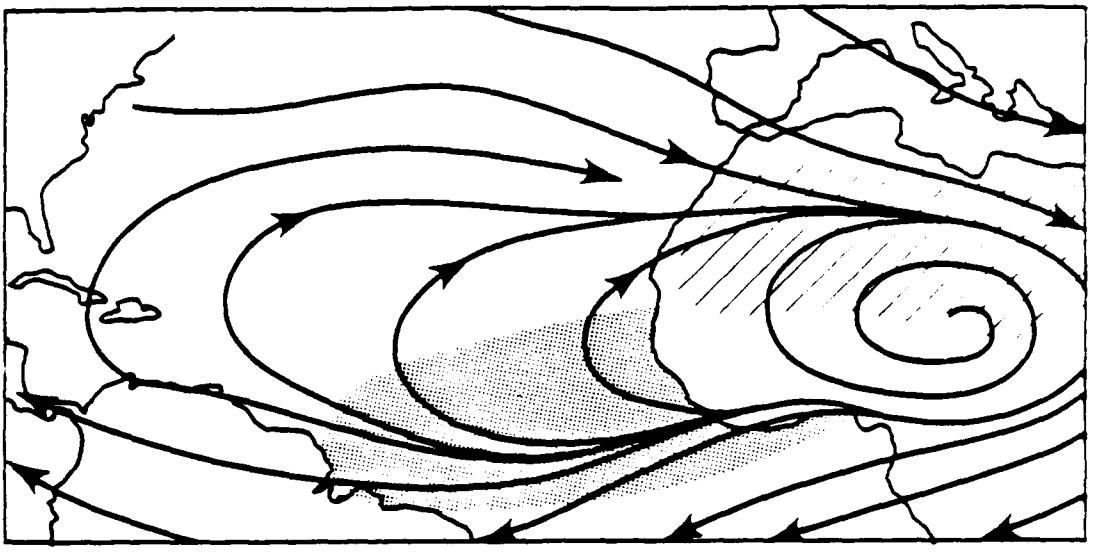

b. Summer.

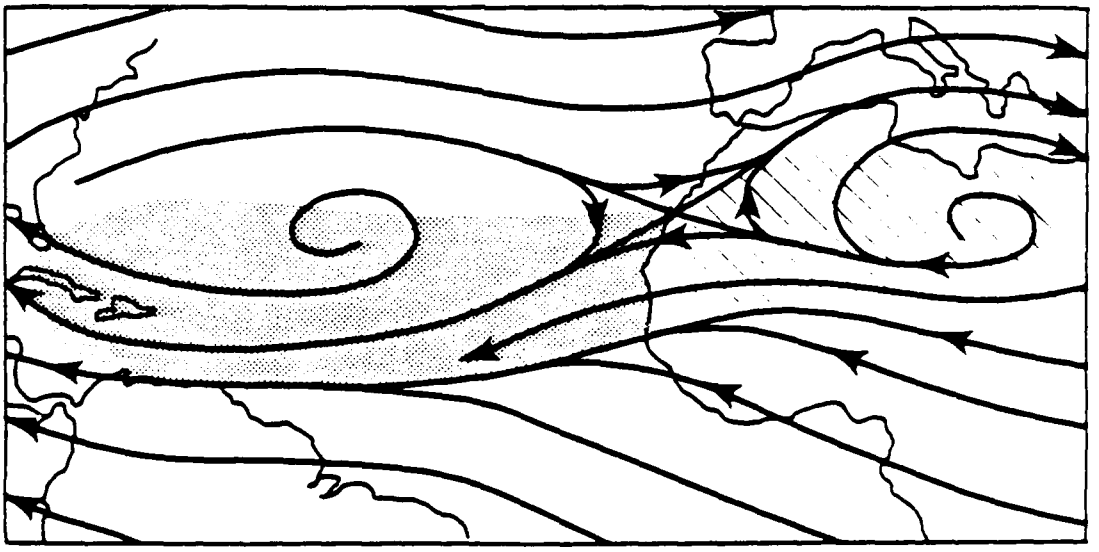

Figure 2. Average Saharan plume positions and mean 700 mbar (∿ 3 km) streamline fields for winter and summer. (Location of Sahara indicated by hatching.)

sistent easterly jet stream at midtropo spheric levels and (2) intense heating of the desert surface by solar radiation. As air masses moving with the easterly current cross the desert, they are rapidly warmed from below by contact with the heated surface. Widespread, vigorous dry convection develops, effectively mixing the warm air near the surface to higher levels. As a result, a warm, nearly isentropic turbulent mixed layer forms, gradually deepening as the air mass proceeds westward. As this deepening continues, some of the horizontal momentum contained in the easterly jet is carried to lower levels through the neutrally stable mixed layer. Surface wind speeds increase and dust lofting ensues. The result is a Saharan dust storm. (The precise conditions necessary for the initiation of dust lofting from the surface are discussed in Sec.3.)

The same convective thermals that trigger a dust storm also mix the dust vertically. This vertical transport continues until the air mass reaches the Atlantic. The mixed layer is often completely dust filled and can extend to 6 km in altitude [Carlson and Prospero, 1972]. Potential temperatures within the layer are quite high (~316 or 317 K in July), and nearly constant with height. During summer, this region is usually dominated by a strong high-pressure system, and the air above the layer can be warmer. Consequently, a weak capping inversion forms, effectively trapping the dust below it and inhibiting further deepening of the mixed layer.

Saharan plume dust concentrations over land are roughly 700 $\mu g/m^3$ [Westphal, Toon, and Carlson, 1987]. Assuming a constant mass concentration to 4 km, the total column density is 2800 kg/km^2—roughly 250 times the average Northern Hemisphere background dust burden [Junge, 1979]. The source areas—chiefly dry lake and stream beds—although relatively small (on the order of 10^3 km^2), are distributed over a very large region [Schütz,1980]. The dust from these multiple sources merges into a single mesoscale plume. A schematic of the early dust plume development and its evolution over the Atlantic is shown in Fig.3.

SAHARAN AIR LAYER.

Once over the ocean, the Saharan dust plume encounters the northeast trade winds. These winds are almost always associated with a strong temperature inversion based between 0.5 and 1.5 km altitude [Riehl, 1979]. The marine air trapped below this inversion is initially dust free and is much cooler (and denser) than the Saharan air. Consequently, as the dusty air contained in the deep mixed layer emerges from the continent, it is forced above the trade wind inversion (Fig. 3). The elevated air mass is called the Saharan air layer (SAL).

The temperature sounding in Fig. 4 shows that the SAL is distinguished by a thick elevated layer of nearly isentropic air in the lower troposphere. The SAL is well mixed—a result of its convective origin over the Sahara, which accounts for the near-uniform vertical distribution of fine (submicron radius) dust particles [Prospero and Carlson, 1972]. The vertical extent of the mixing is limited, however, by the presence of two temperature inversions: the trade wind inversion, which marks the lower boundary, and the capping inversion, based around 6km, which defines the upper boundary. Since these inversion layers are highly statically stable, vertical mixing through them is inhibited. Fine dust is therefore trapped between the inversions and "fumigates" from the SAL into the underlying marine layer at a very slow rate. Consequently, dust concentrations within the marine layer are usually two to four times lower than they are in the SAL [Prospero and Carlson, 1972; Diaz et al., 1976]. Thus the SAL channels the dust in a well-defined layer across the Atlantic.

The SAL is a prime example of how interaction with a weather system can influence long-range dust transport. Nuclear dust clouds originating in mid-latitudes will be similarly influenced. For example, dust masses passing over the oceans could be isolated from near-surface turbulent mixing and removal by low-altitude inversions, especially in summer. On the other hand, large-scale organized precipitation systems are more prevalent in mid-latitudes than in the tropics. It is therefore likely that a nuclear cloud will encounter one of these systems within a few thousand kilometers of its source. Prompt removal of the dust by precipitation scavenging (at least in the lower troposphere) would then ensue. This mechanism will be enhanced if the cloud contains large concentrations of submicron-sized clay particles (especially kaolinite, illite, and montmorillonite). Such particles serve as efficient ice nuclei at temperatures as high as -3°C [Mason, 1971].

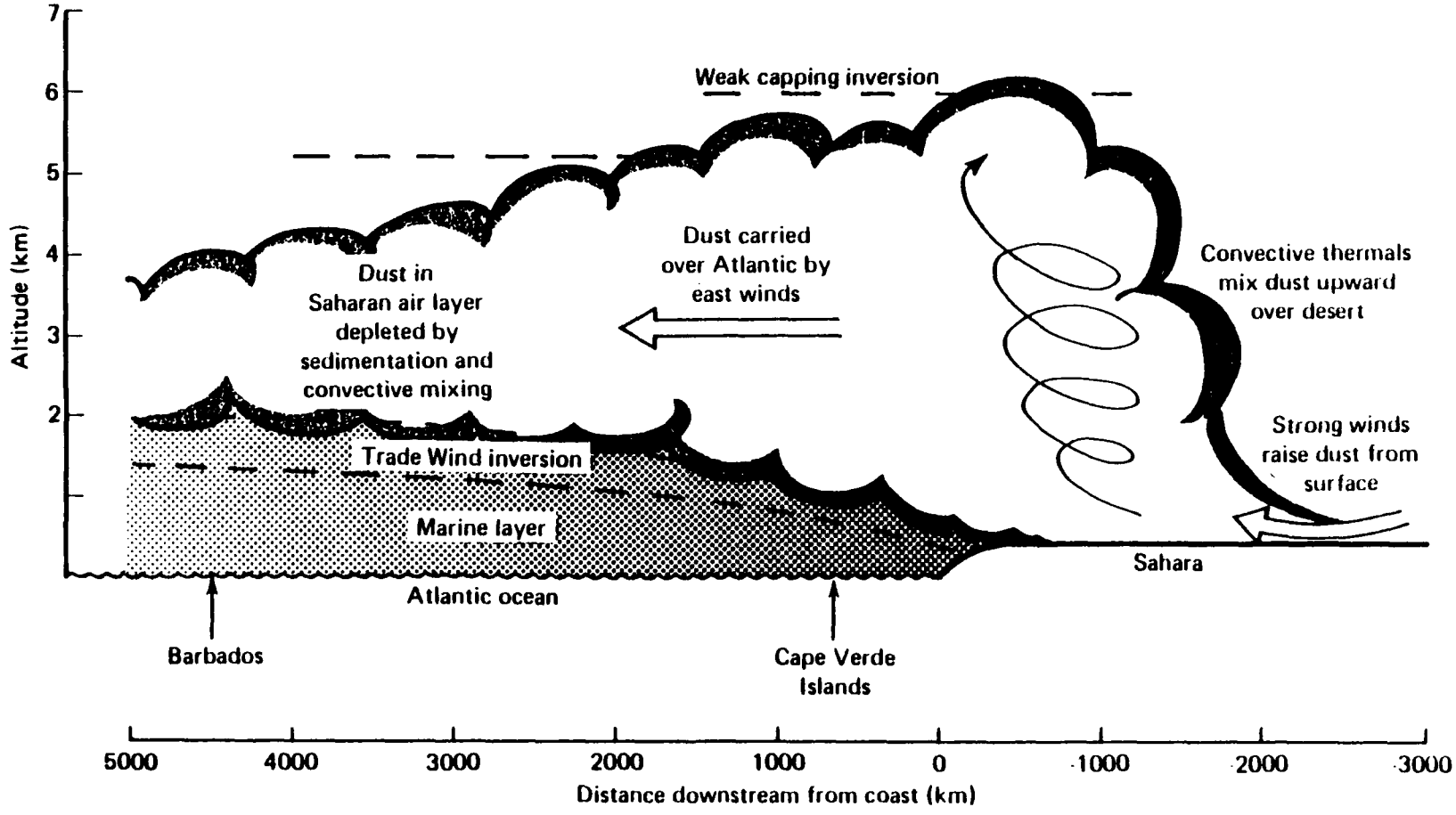

Figure 3. Schematic of major processes involved in lofting, transport, and removal of Saharan dust from atmosphere.

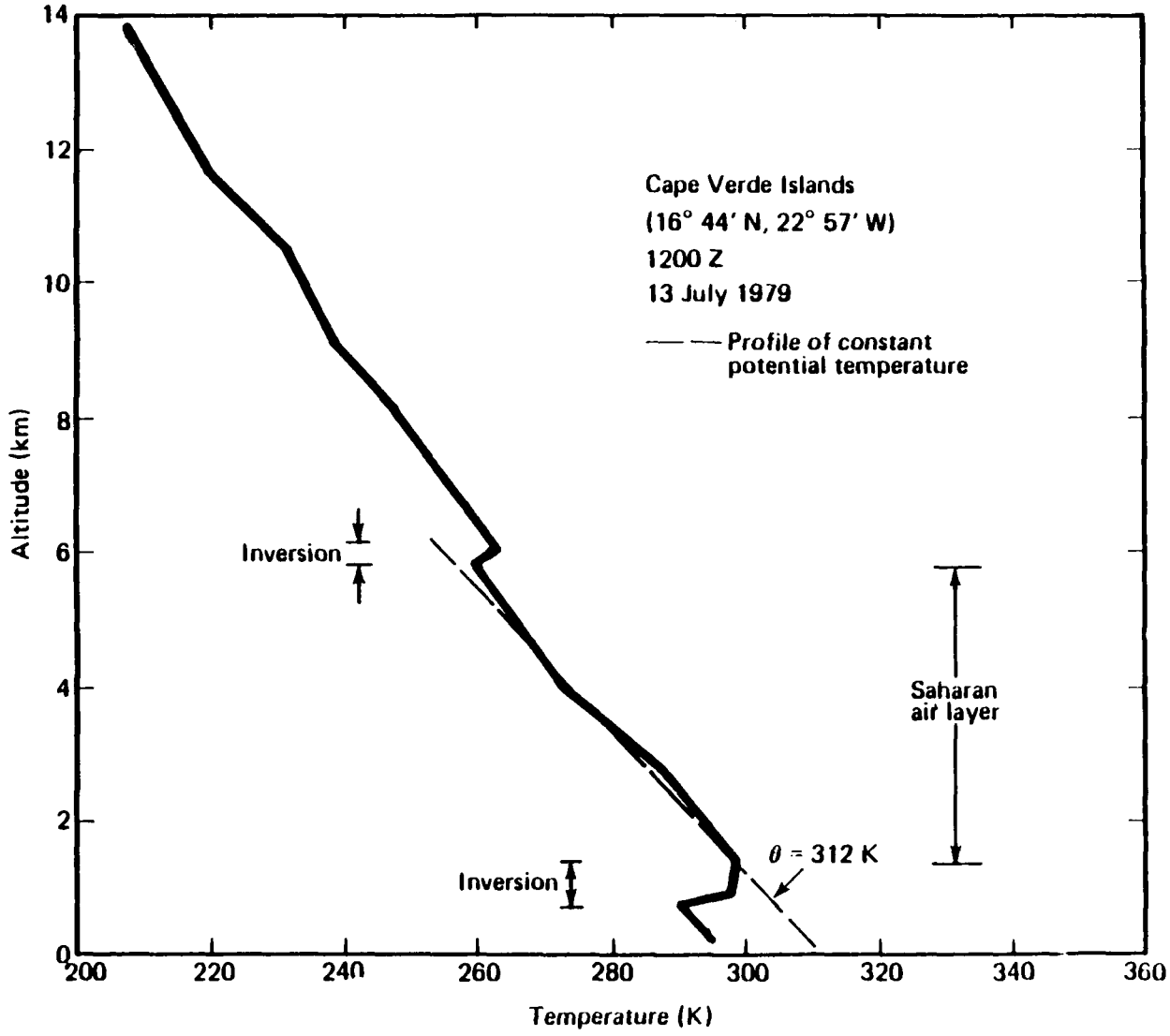

Figure 4. Typical summer temperature profile over tropical north Atlantic near African coast.

MASS DEPLETION RATES.

In the absence of *in situ* depletion measurements, we have analyzed the vertical dust density profiles predicted by two simulations of the Saharan dust plume [Lee, 1983; Schütz, 1980]. By integrating the profiles vertically, the change in column density M (and hence the plume depletion rate R) was determined as a function of distance downstream d. Figure 5 shows M(d) expressed as a percent of the initial column density M_o.

Clearly, the depletion rate decays with distance from the source. Based on Fig. 5, we estimate that roughly one-half the plume mass is depleted in the first 1000 km and that about 70 percent falls out within 200 km. The column density is given by

$$M(d) = M_o\, e^{-d/D(d)} \quad , \qquad (1)$$

where the characteristic "e-folding" distance D is itself a function of d. We find that to a very good approximation

$$D(d) = A + Bd \quad , \qquad (2)$$

where A = 915 km and B = 0.34 km/km in the Saharan plume. Thus D increases linearly downstream. This is somewhat different than the predictions of Lee [1983] and Schütz [1980]. In those models, the plume was assumed to originate either ≈ 1400 km inland over the Sahara [Lee, 1983], or on the coast [Schütz, 1980]. Thus, the meteorological conditions encountered by the simulated plumes were quite different during the early stages of their evolution. Moreover, Schütz and Lee assumed different initial dust concentrations, PSDs, and horizontal transport speeds in their plumes, and treated vertical mixing and surface removal differently. In particular, Lee [1983] assumed the surface deposition velocity to be independent of particle radius. We therefore estimate a somewhat faster depletion than Lee [1983] in the first 4000 km and slower at greater ranges (see Fig.5). This rate is consistent with the mass flux estimates of Ganor and Mamane [1982] and the optical depth/plume mass measurements of Carlson [1979].

From Eqs.(1) and (2), the plume depletion rate following a downstream trajectory is

$$R(d) = -U\frac{dM}{d(d)} = \frac{UM_oA}{(A + Bd)^2}\, e^{-d/D} \quad , \qquad (3)$$

where U is the horizontal transport speed. Assuming M_o = 3000 kg/km² and U = 20 m/s (typical values for the Saharan plume), we find R decays exponentially from an initial value R_o = 236 kg/km²/h as shown in Fig.6. Far from the source (d ≈ 7000 km), the depletion is about two orders-of-magnitude smaller than R_o (R ≈ 2kg/km²/h); this rate corresponds to a surface deposition of only a few microns per year.

PARTICLE-SIZE DISTRIBUTION.

The radiative, optical, and mechanical hazard properties of any dust plume depend not only on the total mass contained within the plume, but also the PSD. Windblown or scoured dust usually comprise a wide range of particle sizes.

Dust distributions representative of near-surface PSDs in the source region (Libya) and at three points downstream are shown in Fig.7. The cumulative mass per unit volume m of all particles of radii less than r is given as function of particle size.[2] Figure 7 shows that (1) the total mass concentration decays very rapidly downstream, (2) with distance from the source, the distribution shifts to smaller particles, and (3) the depletion rate depends strongly on particle size. This is especially obvious when we compare the relative change in dm/d(log r) for radii less than 1μm with that for larger radii. Most of the mass depletion occurs when larger particles (r > 1 μm) fall out. The submicron concentration remains fairly constant (Table 1); these particles are transported long distances—even though the plume top is fairly low. Nuclear clouds rising to the upper troposphere would travel even farther and, if they penetrate into the stratosphere, could remain aloft for years. (Volcanic plumes provide a good analogue for such stratospheric transport.)

2. The mass distribution dm/d(log r) is proportional to the number distribution dN/dr by $dN/dr = (3/4\pi r^4 \rho_p \ln 10)\,[dm/d(\log r)]$, where ρ_p is the particle density.

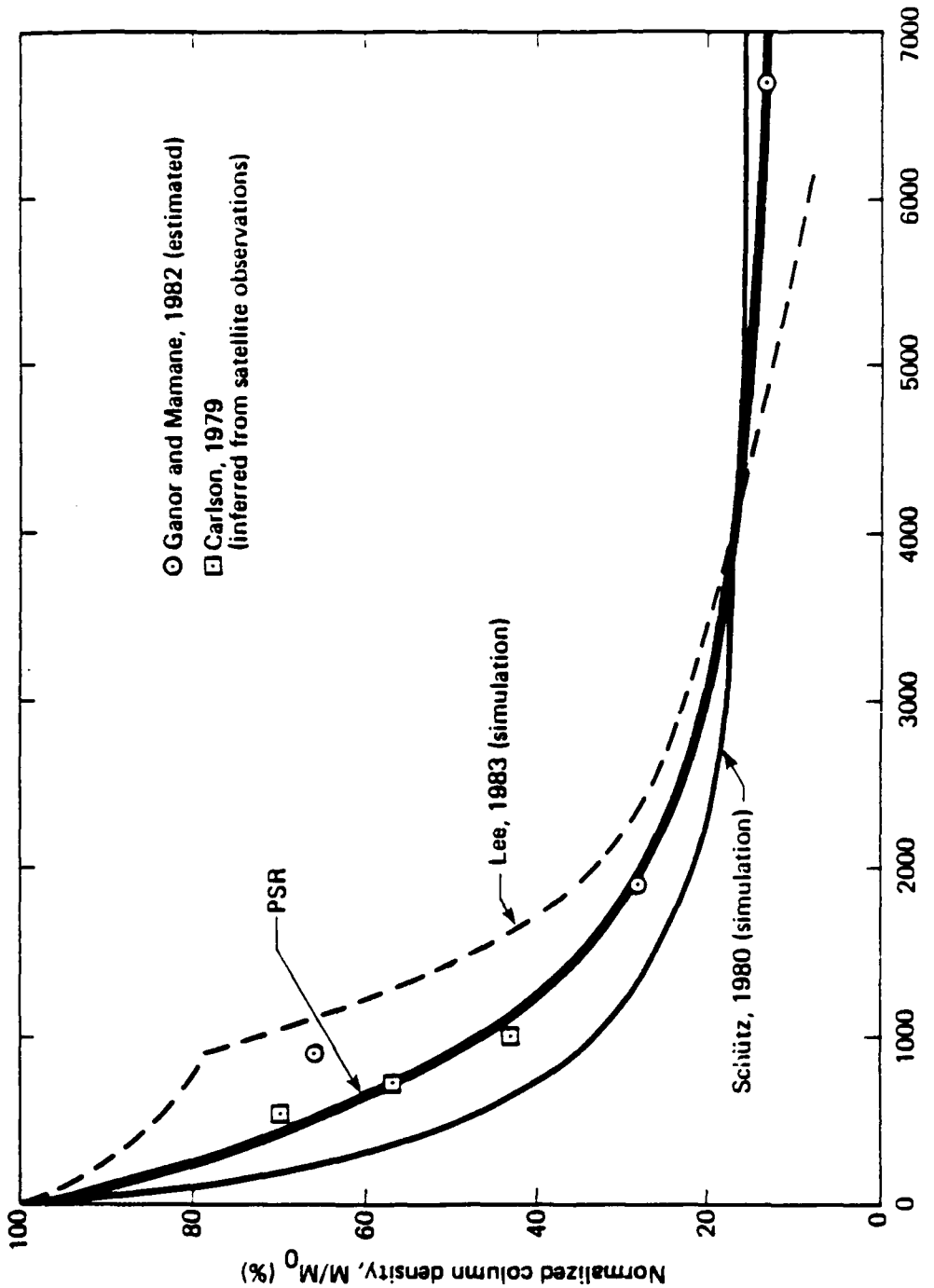

Figure 5. Normalized column density in Saharan plume as function of distance downstream.

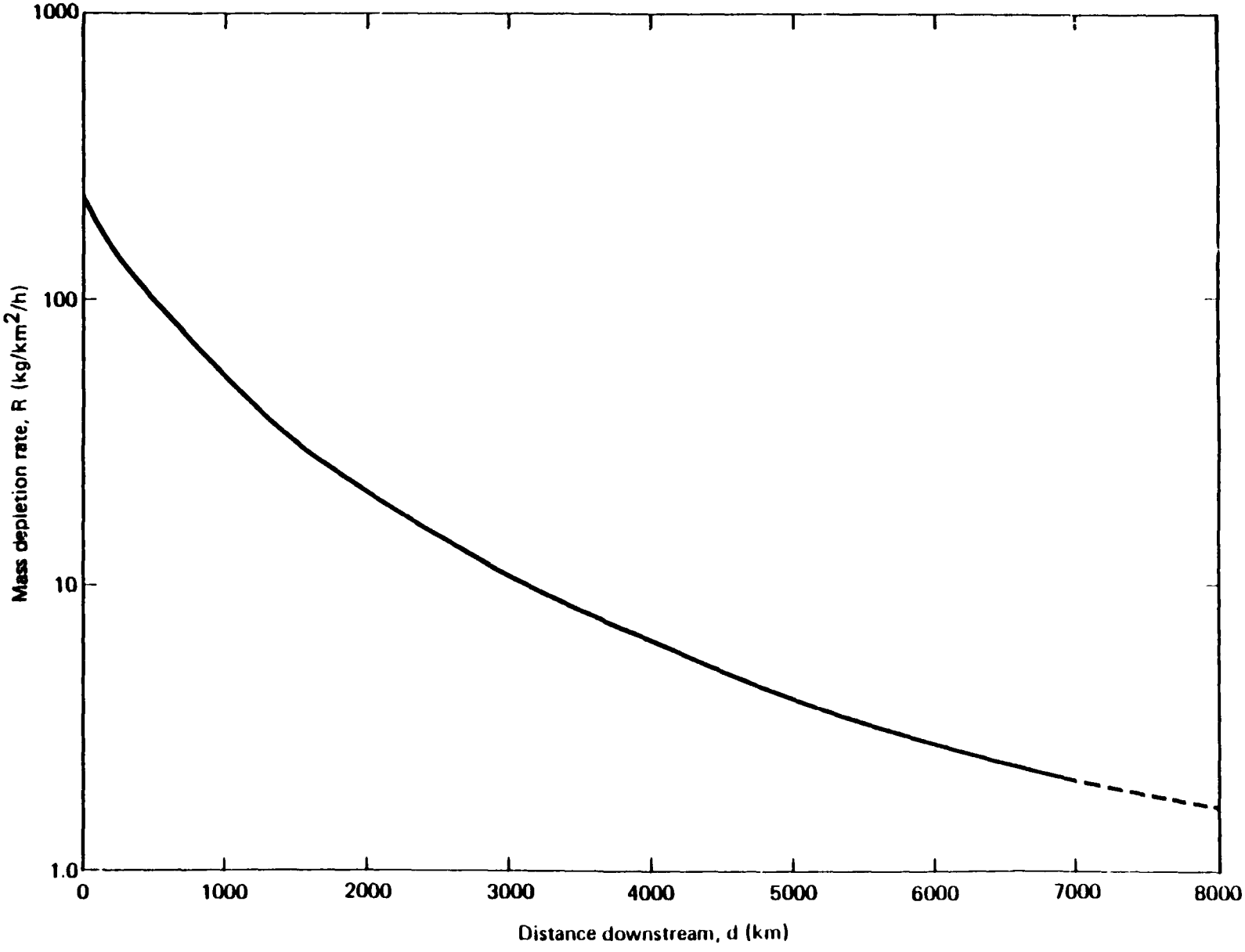

Figure 6. Mass depletion rate in Saharan plume as function of distance downstream.

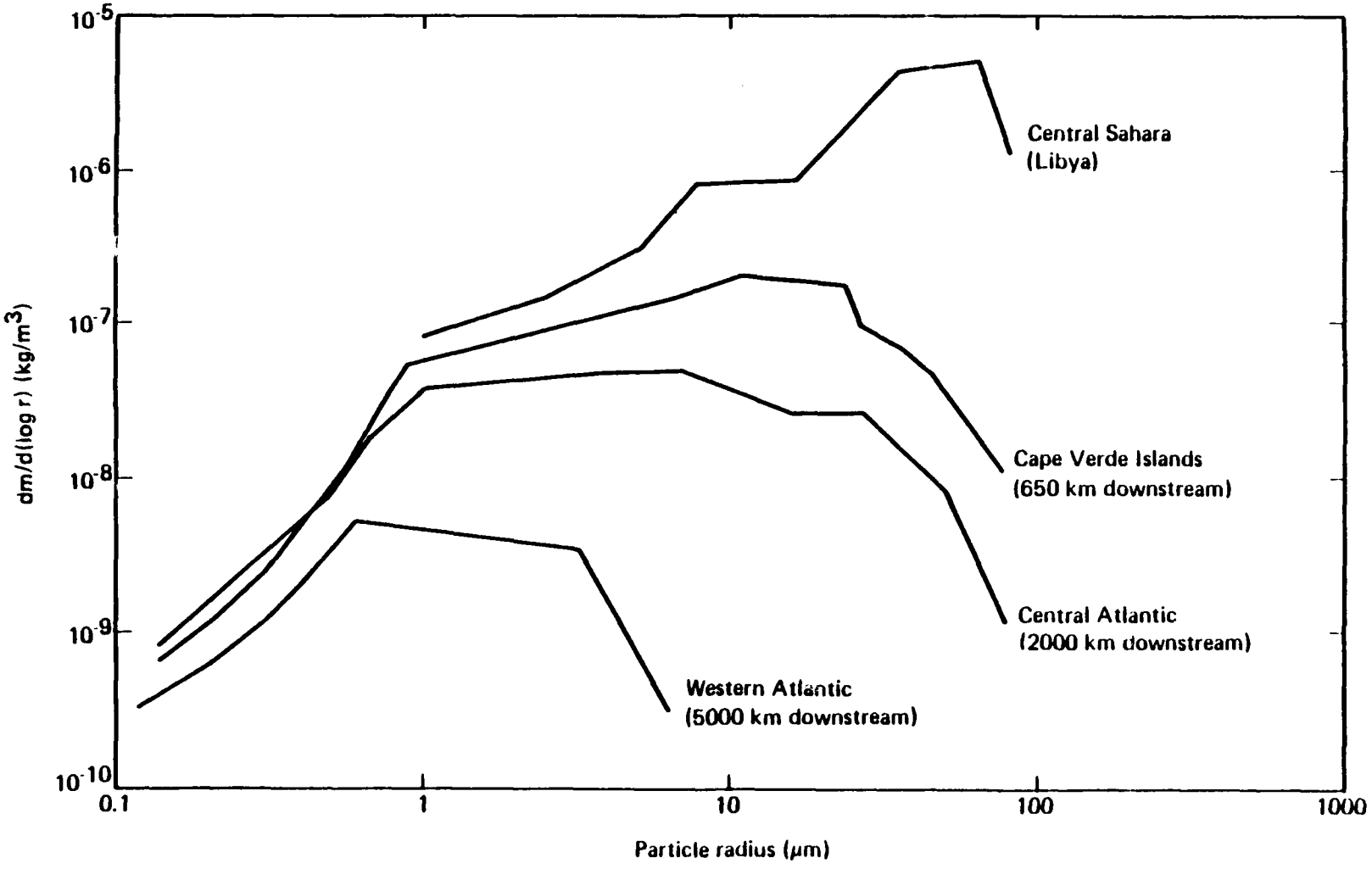

Figure 7. Representative particle-size distributions in Saharan plume.

Table 1. Mass partitioning in Saharan dust observations.

Observation Site	Total Mass Concentration ($\mu g/m^3$)	Percent by Mass with Radii Less Than 1 μm	Mass Concentration of Submicron Portion ($\mu g/m^3$)	Median Radius (μm)
Central Sahara	~2800	~1	~28	~38.6
Cape Verde Islands	215	6	13	8.9
Central Atlantic	75	11	8.3	4.2
Western Atlantic	5	44	2.2	2.8

Saharan plumes are wind lofted (scoured) and therefore consist mostly of smaller sized ($r < 1$ μm) particles—at least at later times. The scouring mechanism for nuclear clouds is much stronger (although transient) and initially a wider spectrum of particle sizes is lofted. However, the largest particles fall out promptly. At later times, nuclear cloud PSDs may therefore be similar to the Saharan distributions.

REMOVAL MECHANISMS.

A dust particle can be removed by sedimentation, mixing to the surface by turbulence, scavenging by precipitation (wet removal), or by combining with one or more particles to form a larger aggregate (coagulation). At least two of these mechanisms—sedimentation and turbulent mixing—play key roles in Saharan plumes. Sedimentation, which depends on the terminal velocity of a particle and hence on its size, is responsible for the rapid removal of large ($r > 1$ μm) particles. Turbulent mixing is effective for particles so small that their sedimentation is significantly retarded by viscous forces and is responsible for the gradual removal of submicron-radius particles.

Wet removal apparently has little effect on Saharan plumes, since the transport occurs mostly in the dry air between successive westward propagating wave disturbances [Carlson and Prospero, 1972]. This is quite different from the situation expected for mid-latitude nuclear clouds, where rain systems are more frequent and wet scavenging in the troposphere is likely.

Coagulation has a noticeable impact on the evolution of the Saharan PSD only when turbulent mixing and, especially, sedimentation are not dominant [Lee, 1983]. Rapid depletion by sedimentation and turbulent mixing lessens the development of large particles by coagulation (see Fig. 8). For Saharan plumes, coagulation is usually not a significant factor. There have been measurements made over the Atlantic, however, that show particles too large to have survived depletion by sedimentation and turbulent mixing. Particles in excess of 100-μm radius have been sampled in the marine layer over the Canary Islands [Goude-Gaussen et al., 1987]. Coagulation obviously is responsible. Observations of anomalously large particles have also been made over the Cape Verde Islands [Glaccum and Prospero, 1980] and the central Atlantic [Carder et al., 1986].

Clearly, some mechanism other than direct transport from the Sahara is responsible for such "ultragiant" particles. One possibility is local "cloud processing," which may occur when small, initially uncoagulated particles from the SAL pass through underlying stratus decks [Westphal, Toon, and Carlson, 1987]. Such a moisture-aided coagulation mechanism would be important when dust clouds encounter nonprecipitating clouds. But this is speculative; the presence of ultragiant particles far downstream re-

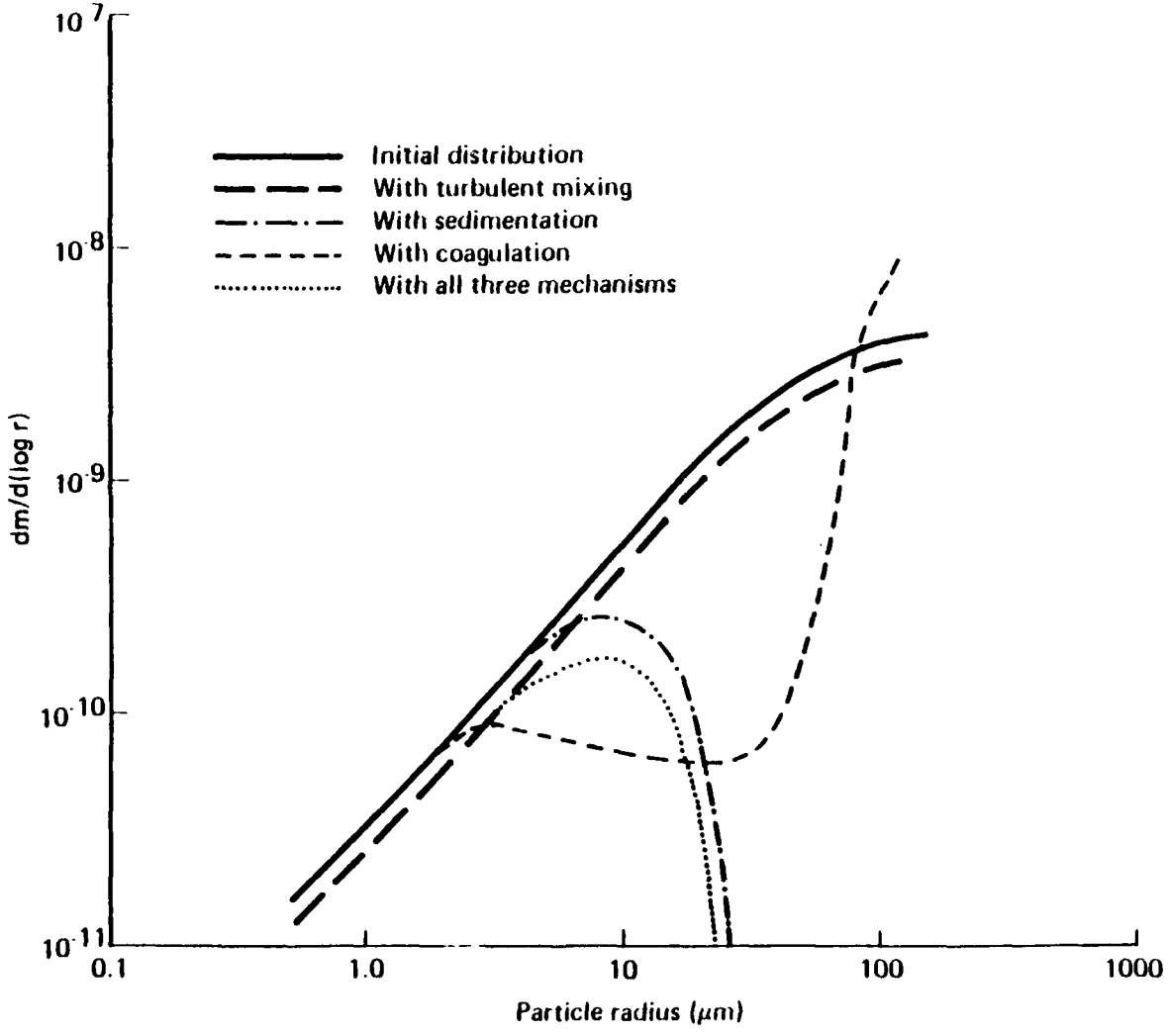

Figure 8. Effect of various dust removal mechanisms on Saharan dust particle-size distribution after 48 h simulation time.

mains unexplained. The possibility that large particles could exist far from the source is relevant for nuclear clouds since these particles (especially for $r > 20$ μm) could cause the most mechanical damage to flight vehicles. Moreover, in the mid-latitudes, the opportunity for formation of larger particles by cloud processing is probably much greater than in the Saharan dust systems.

RADIATIVE EFFECTS.

Dust is an obscurant. A beam or signal through a cloud of dust is attenuated by absorption and scattering. The amount of this attenuation is given by Beer's law, which expresses the ratio of the beam irradiance I_λ at wavelength λ emerging from the cloud to the incident irradiance $I_{\lambda 0}$:

$$\left(I_\lambda / I_{\lambda 0} \right) = e^{-\tau_\lambda} \quad . \tag{4}$$

Here τ_λ is the spectral optical depth. For a vertically oriented beam, it is defined as

$$\tau_\lambda = \int_0^h \left(k_{\lambda,a} + k_{\lambda,s} \right) dz \quad , \tag{5}$$

where z is the vertical coordinate, h is the cloud thickness, and k_λ and $k_{\lambda,s}$ are the volume spectral absorption and scattering coefficients, respectively.

In Saharan plumes, the particles are sufficiently large compared to solar wavelengths that the optical depth is linearly related to the column mass M by

$$\tau_\lambda = M / \alpha \quad , \tag{6}$$

where α is constant equal to 3750 kg/km^2 near Africa and roughly 1500 kg/km^2 over the western Atlantic [Carlson and Caverly, 1977]. This formula was used to derive the satellite-observed column densities shown in Fig. 5.

Figure 9 maps τ_λ at a solar wavelength ($\lambda = 0.66$ μm) determined from satellite observations during a particularly severe Saharan dust episode. Note the elongated pattern of the isopleths. The largest values ($\tau_\lambda > 3.5$) are located near the Mauritanian coast where the plume first emerges. As the dust is transported westward and spreads laterally, measured optical depths lessen, consistent with dispersion and depletion of the plume. Values of τ_λ in excess of 2.0 cover an area of about 3×10^5 km^2. These optical depths are very high—background values in relatively dust-free regions seldom exceed 0.25—and solar irradiance at the surface is reduced by 86 percent. Such obscurations are consistent with surface dust concentrations of 200 μg/m^3 measured at Sal Island (in the Cape Verde Islands). At these concentrations, visibility is reduced to the point that it is impossible to distinguish cloud from sky [Carlson, 1979]. The outbreak shown in Fig.9 was exceptionally massive; a more typical value of τ_λ in Saharan plumes is 1.5 [Carlson, 1979]. A nuclear cloud, however, would be at least twice as thick as the Saharan plume at these early times. The optical depth would also be twice as large. The large outbreak shown in Fig. 9 is therefore more representative of the optical depths expected in a nuclear dust cloud.

The large optical depths associated with some Saharan dust storms imply significant modification of local weather, especially near the source region. Even several hundred kilometers south of the Sahara (Nigeria) visibilities during winter dust episodes can drop to less than 0.5 km at the surface [Brinkman and McGregor, 1983]. During these episodes, visibility tends to be low during the day and improves at night. Thermal convection from the heated ground helps fumigate lofted dust to the surface. Reductions in surface temperatures are associated with the low visibilities. Daily maximum temperature changes up to 6°C have been reported [Brinkman and McGregor, 1983].

In Saharan plumes absorption plays a minor role compared to scattering. The magnitude of the absorption is determined by the molecular structure and composition of the dust particles, and is measured by the imaginary part of the index of refraction n_I. This dimensionless quantity is related to the volume absorption coefficient $k_{\lambda,a}$ by

$$n_I = \frac{\lambda \, k_{\lambda,a}}{4\pi} \quad . \tag{7}$$

For Saharan dust, n_I is very small: Measured values at solar wavelengths range from about 0.001 to 0.02, with an average around 0.005 [Carlson and Benjamin, 1980]. Such values are typical of silicates. By comparison, smoke, which is a

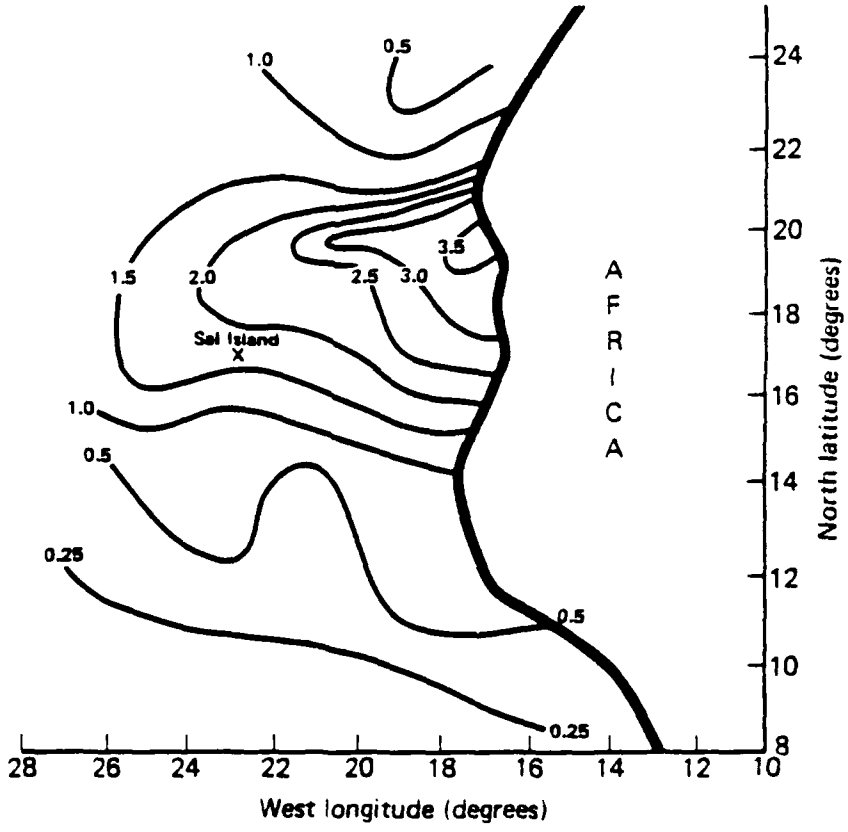

Figure 9. Observed dust optical depths (λ = 0.66 μm) in Saharan plume for 0942 GMT, 30 July 1974.

much more efficient absorber of solar radiation, has an imaginary index of refraction around 0.1 or larger [NRC, 1985]. The low absorptivity of Saharan dust is due in part to its very low organic content. Saharan aerosols contain less than 2 percent mass of carbonaceous material [Jaenicke and Schütz, 1978]. This is much lower than the organic fraction found in most other dust aerosols around the world (supporting the view that the Sahara is "organically dead.") Nuclear dust clouds are likely to be more absorptive than Saharan plumes, since many U.S. and USSR silo fields are located on thick, organically rich prairie or steppe soils (mollisols or *chernozem*). Stronger absorption in these clouds would increase atmospheric warming in the upper troposphere and could induce a "self-lofting" mechanism similar to that expected for smoke clouds. This has not been detected in the largely silicate Saharan plumes.

Scattering in dust clouds is a strong function of particle size. In the Saharan plume, the effective scattering radius r_s is usually quite large compared to solar wavelengths ($\lambda_{peak} \approx 0.5$ μm). For example, over the eastern Atlantic, $r_s \approx 2$ to 5 μm [Carlson and Caverly, 1977]. As a result, the scattering coefficient $k_{\lambda,s}$ is large, and most of the incident solar radiation is reflected or backscattered. Further downstream, however, the large particles responsible for reflection are depleted and $r_s \approx \lambda_{peak}$. Scattered radiation is then directed primarily in the *forward* direction (Mie scattering); $k_{\lambda,s}$ therefore decreases and the optical depth due to scattering is reduced.

In a nuclear dust cloud, scattering depends on the characteristic particle size. For a cloud with an initial PSD similar to a Saharan distribution, we expect that $k_{\lambda,s}$ at solar wavelengths would decrease downstream as large particles are depleted and the scattering passes from the geometric to the Mie regime. It is possible, however, that nuclear clouds would have a greater initial mass fraction of submicron-size particles due to condensation of vaporized soils. Mie scattering would then dominate, and the nuclear cloud would therefore be less reflective than the Saharan plume.

SECTION 3

LOFTING MECHANISMS

VERTICAL MASS FLUX.

Winds at the earth's surface exert shear stresses on the ground. If the stress is large enough, material is raised from the surface and transported by the airstream (saltation). The vertical mass flux F_z is proportional to the wind speed as

$$F_z = CU_*^n \quad . \tag{8}$$

where C and n are empirical constants and U_* is the friction velocity for a turbulent shear layer [Gillette, Blifford, and Fenster, 1972] computed from:

$$U_* = k\left(U_2 - U_1\right) \ln\left(Z_1 / Z_2\right) \quad . \tag{9}$$

Here $k \approx 0.4$ is the Von Karmann constant and U_1 and U_2 are wind speeds measured at heights Z_1 and Z_2, respectively.

The experimentally measured dependence of F_z on U_* for three desert soil types—sand, loam, and clay is summarized in Fig. 10. The vertical mass flux increases nonlinearly with increasing U_* and depends on soil type. A least-squares fit by Westphal, Toon, and Carlson [1987] suggests that

$$F_z \approx 2 \times 10^{-10} U_*^3 \ \text{kg/m}^2\text{/s} \quad . \tag{10}$$

where U_* is in centimeters per second. Thus n = 3 in Eq.(8). The vertical mass flux of particles from the surface is therefore proportional to the flux of kinetic energy delivered to the surface [Gillette, 1980]. However, shock tube experiments [Hartenbaum, 1971] and theoretical work [Mirels, 1984] show that $n \approx 1.1$ to 1.2 at wind speeds more typical of a nuclear environment [$U_* = O(10^2)$ m/s]. Both Hartenbaum's [1971] results and Mirels's [1984] are for highly idealized conditions (e.g., flat, noncohesive soil surfaces) rather than natural soils. The greater scouring rates for Saharan dust may also result from the steady winds, whereas in a nuclear pulse, peak velocities are large but transient.

The measurements in Fig. 10 also show a threshold friction velocity U_{*th} below which no erosion occurs. Moreover, the value of U_{*th} depends strongly upon the soil type, as indicated by the vertical dashed lines in Fig. 10.

THRESHOLD VELOCITY.

Soil types and conditions vary widely depending on location, time of year, and, in deserts, the diurnal cycle. The threshold friction velocity required to initiate dust lofting also varies, although the dependence of U_{*th} on soil type is not immediately obvious. For example, clay soils (which contain a large number of very fine submicron particles) have higher threshold velocities than sand. The distinction is important since U_{*th} determines whether dust storms develop.

Values of U_{*th} for a variety of soil types and conditions in the Mojave Desert have been experimentally determined [Gillette et al., 1980]. Both undisturbed and disturbed soils were tested. The results are presented in Table 2. Disturbed soils generally have lower threshold velocities than undisturbed soils; the presence of clay or salts tends to increase U_{*th}, especially if a crust is present. Even a thin (0.5-cm thick) and weak (modulus of rupture $\approx$ 0.7 bar) crust (e.g., typical of undisturbed dry lake beds) can protect the underlying soil from all but the strongest winds [Gillette et al., 1982]. The strength of a crust is highly dependent on the amount of mica-free clay present, although exchangeable sodium and calcium carbonate also increase cohesiveness. Scouring thresholds are also increased for freeze conditions and snow coverings, water or salt (especially in crystalline form) in the soil, aggregation or "clumping" of particles, a high clay content, and obstacles which increase surface roughness (e.g., pebbles, boulders, vegetation).

Modifying the threshold velocity to account for the nuclear environment is clearly necessary. Intense thermal radiation can fuse soil particles and form a thin but strong glassy crust. On the other hand, thermal radiation also vaporizes soil water, leading to a decrease in cohesiveness and in U_{*th}. In some cases, the rapid vaporization is explosive, and can disrupt a preexisting crust. Shock loading at the surface can also break soil crusts (spalling) and produce large aggregated soil clumps. Such clumps have much larger aero-

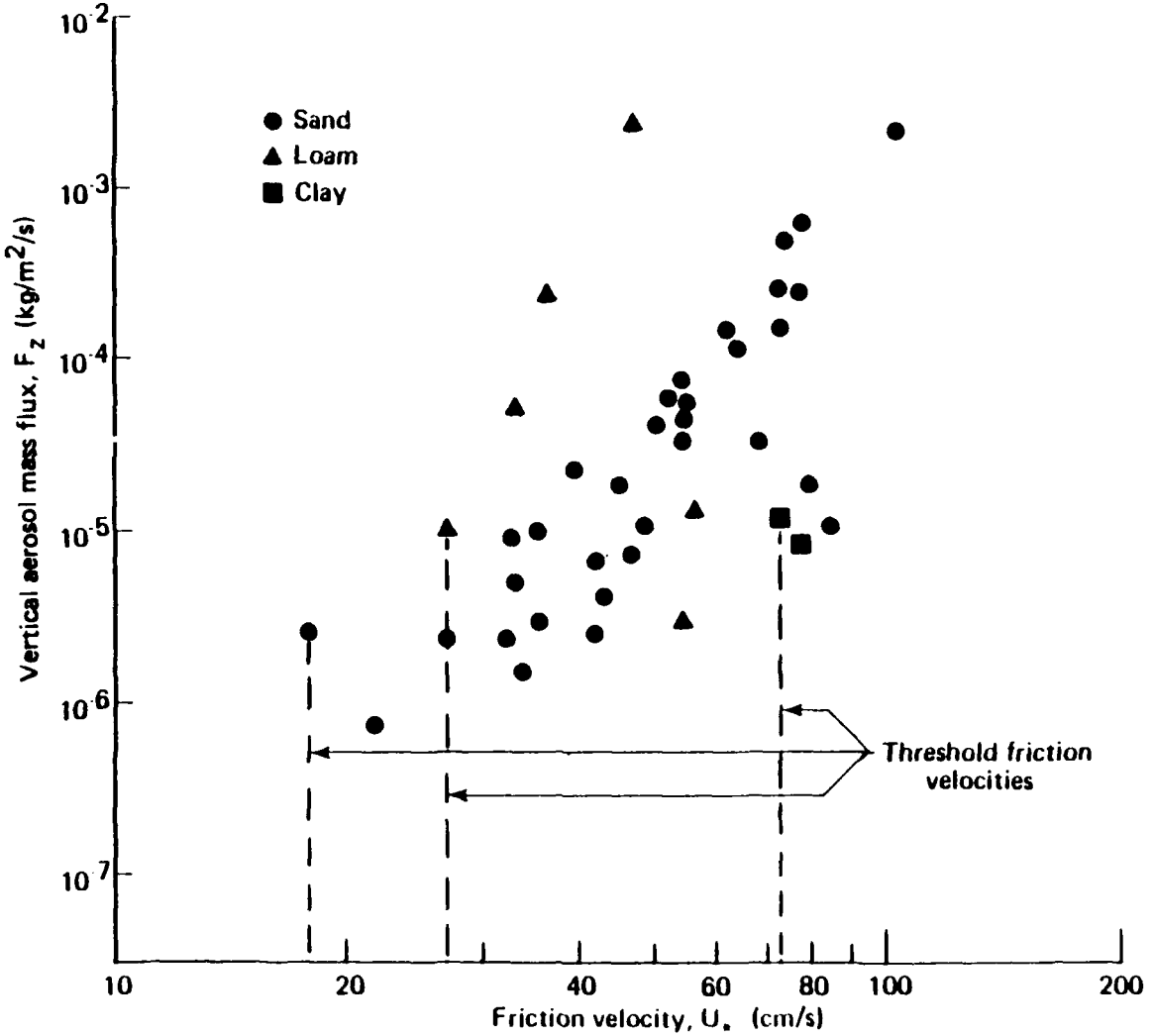

Figure 10. Dependence of vertical dust mass flux from surface on friction velocity

Table 2. Threshold velocities for various soil types.

Soil Type	Approximate Threshold Velocity Range (m/s)
Disturbed soils with < 50% clay content and sparse pebble cover (< 20% surface area)	0.20-0.40
Tilled bare sand	0.25-0.40
Disturbed pebbly soils	0.40-0.65
Bare clay with naturally disaggregated particles	0.45-0.70
Disturbed soils with high salt or clay content	0.40-1.50
Undisturbed sandy soils	1.40-2.00
Undisturbed soils with high clay content and surface crusts	> 1.5
Salt-crusted soils	> 1.5
Soils covered by coarse (> 5 cm) pebbles	> 1.8

Source: Gillette [1980].

dynamic cross sections than individual soil grains and are therefore preferentially lofted from the surface (assuming large enough U_*). However, they are massive, do not remain lofted for long, and break into smaller pieces at the surface [Patterson and Gillette, 1977]. The soils can then be scoured and carried to high altitude with the rising fireball.

SECTION 4

NUCLEAR DUST ANALOGUE

The Saharan dust plume transports large dust masses thousands of kilometers, although in a cloud of limited vertical extent. Figure 11 compares predicted maximum dust concentrations at ten hours for two nuclear exchange scenarios[3] with that for a natural Saharan plume. The Saharan plume is clearly a lower tropospheric phenomenon, while nuclear clouds involve the entire troposphere and part of the stratosphere. Nevertheless, the dust concentrations within nuclear and Saharan dust clouds are similar at low altitudes (below 3 km).

Other aspects of the Saharan plume are compared with nuclear clouds in Table 3. Clearly, the analogue is not perfect: Soils in the source regions are dissimilar, nuclear sweepup is more energetic (and may involve blast effects), and removal mechanisms are different (especially in middle latitudes). There are similarities however, especially in the long-range transport and long-time cloud depletion.

LOFTING MECHANISMS.

Low-altitude nuclear explosions loft dust into the atmosphere by one of two mechanisms: (1) sweepup by the strong, blast-induced winds and (2) cratering. For detonations with a scaled height of burst (SHOB) less than about 70 ft/MT$^{1/3}$, both of these mechanisms contribute to the lofted dust mass. For greater SHOBs, only sweepup is a factor [NRC, 1985].

The physics of sweepup are poorly understood. Generally, experimental studies have been conducted under highly idealized laboratory situations (e.g., Hartenbaum, 1971). Natural soils and conditions have not been extensively studied under nuclear sweepup circumstances (thermal irradiation of the surface, high blast overpressures, high-velocity transient winds, etc.). Natural dust lofting processes provide a simulation, if only partial, of nuclear sweepup.

Saharan dust clouds vary with the source region and time of year. The rate at which dust is lofted or scoured from the surface strongly depends on the soil type and its condition (e.g., whether or not it is crusted, the amount of clay and salt, the presence of vegetation). Moreover, the total mass lofted and fraction transported long distances depends on the soil size distribution. These factors are clearly important for the weak Saharan forces, but may also influence the characteristics of lofted nuclear dust clouds.

Silo fields, located primarily in regions dominated by thick, organically rich soil deposits (e.g., the Great Plains), experience winter freezes and seasonal changes in vegetation. The susceptibility of such target area soils to sweep-up is clearly quite different from that of arid (Saharan) soils. Nevertheless, large dust clouds are swept up by surface winds in both cases; and far from the source, the depletion can be similar.

LONG-RANGE TRANSPORT. THE DEVELOPMENT OF THE

Saharan plume requires specific atmospheric conditions. These conditions also make it possible for the dust to be carried long distances. Without the channeling influence of the Saharan air layer over the tropical Atlantic and in the absence of wet removal, it is doubtful that much dust would survive in the atmosphere as long as it does. Nuclear dust clouds are likely to be subject to a full range of meteorological conditions. In midlatitudes, dust depletion rates are higher principally due to organized precipitation systems. Thus, the Saharan plume probably represents an upper limit to dust cloud transport and longevity in the lower troposphere.

DEPLETION RATES.

Although there are obvious differences, far from the source region (or target area), mass depletion for Saharan and nuclear dust clouds should be similar. For the two cases, the constants in Eq.(1) are different. Nuclear burst lofting mechanisms (scouring and fireball upsweep) are much stronger than in the Saharan case, and the initial lofted mass is dominated by more massive par-

3. Scenario A assumes a U.S. laydown on the Soviet Union involving 1500 MT total yield with 500 MT in surface bursts. In scenario B, a Soviet counterforce attack on the U.S. is assumed involving several thousand megatons of surface and near-surface bursts, including several large (20MT) detonations (see Yoon et al., 1986).

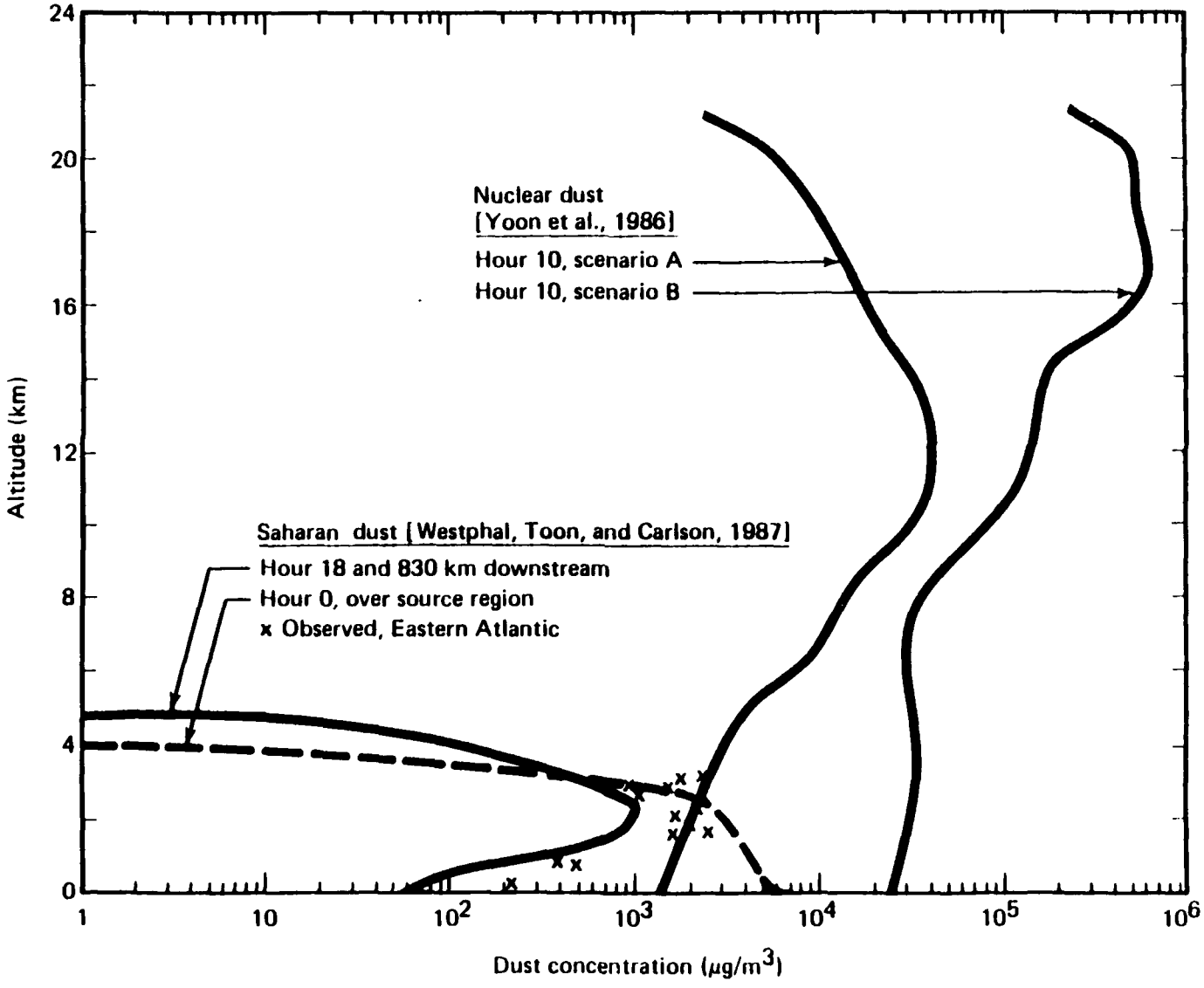

Figure 11. Comparison of simulated vertical dust concentration profiles in Saharan plume and nuclear dust cloud.

Table 3. Comparison of Saharan and nuclear dust plumes.

Characteristic	Saharan Dust	Nuclear Dust
Composition	Quartz grains (large particles) Clay (small particles) Organic content < 2% by mass	Variable (depends on surface) Organic content > 5% by mass
Soil cohesion	High (salt-crusted and clay soils) Low (sand)	Seasonally dependent
Lofting mechanisms	Sweepup (U ~ 1 m/s) Convective thermals	Sweepup (U ~ 100 m/s) Cratering (SHOB < 70 ft/MT$^{1/3}$) Fireball rise
Source strength	8–10 Tg per storm 10^3–10^4 km^2	~ 25 Tg (150 silos, 0.5 MT each) ~ 4 x 10^4 km^2
Maximum altitude	6 km	> 20 km (higher if multiburst)
Mass concentration (maximum)	Surface: 10^3–10^4 μg/m^3	Surface: 10^3–10^5 μg/m^3
	Aloft: ~ 10^3 μg/m^3 (3 km)	Aloft: 10^4–10^6 μg/m^3 (tropopause)
Submicron mass fraction	~ 1% (source region) 45% (western Atlantic)	19% (stabilized Johnie Boy cloud)
Optical depth (visible wavelengths)	~ 1.5	> 3.0
Removal mechanisms	Sedimentation Turbulent mixing	Precipitation scavenging Sedimentation
(coagulation minimal)	Turbulent mixing	(coagulation may be significant)
Removal rate	70% mass in first 2000 km	> 70% mass in first 2000 km (lower troposphere only)

ticles. The initial depletion is there fore larger. Moreover, the largest particles are rapidly depleted so that the column density M decays more rapidly. Thus, the e-folding distance D is smaller. Finally, far downstream, where depletion is dominated by submicron-size particles, M is likely to be larger due to the greater initial submicron-size concentrations in the stabilized nuclear cloud. The larger mass in submicron particles in the nuclear cloud can result, for example, from fireball vaporization and recondensation processes or from efficient pulverization of soil aggregates by the blast.

Since the nuclear cloud is likely to be much thicker and the PSD different, we calculate the column density M as follows:

$$M(d) = - U \int_{o}^{d} R(\zeta)\, d\zeta \quad , \qquad (11)$$

where

$$R = -\frac{dM}{dt} = \int_{o}^{z_{top}} \frac{\partial}{\partial z} \Phi(z)\, dz \quad . \qquad (12)$$

Here U is the horizontal transport speed, $\Phi(z)$ is the vertical mass flux crossing altitude z, and z_{top} is the maximum plume altitude. Horizontal spreading and vertical wind shear is neglected. For a given PSD, i.e., dm/d(log r), the vertical mass flux is:

$$\Phi(z) = \int_{\theta_{min}}^{\theta_{max}} \left[V_s(\theta,z) \frac{dm}{d\theta} \right] d\theta \quad , \qquad (13)$$

where $V_s(\theta,z)$ is the sedimentation velocity (a function of particle radius r), $\theta = \log(r)$, and θ_{max}, θ_{min} correspond to the upper and lower radii bounds. Substituting Eq.(12) into Eq.(11) and using the condition $\Phi(z_{top}) = 0$ gives

$$R = \int_{\theta_{min}}^{\theta_{max}} \left[V_s(\theta) \frac{dm}{d\theta} \right]_{surface} d\theta \quad . \qquad (14)$$

Thus R is equivalent to the mass flux at the surface.

We use Eqs.(11), (12), and (13) to compute M as a function of d for several hypothetical nuclear PSDs. Initial dust concentrations and PSDs are specified and assumed to be independent of altitude throughout the troposphere ($z \leq 10$ km); no stratospheric loading is assumed. The troposphere is divided into ten layers ($\Delta z = 1$km). Particles in seven radius bins [$r_{min} = 0.01\mu m$, $r_{max} = 32\ \mu m$, $\Delta(\log r) = 0.5$] fall through the interfaces between these layers at a sedimentation speed V_s (proportional to $r^{1/2}$) given by Stokes's law. Separate mass balances are kept for each layer. As each layer "feeds" dust into the neighboring layer below it (and receives dust from the layer above), the spectral mass concentration dm/d(log r) changes. The net change in column density for each layer over a small time interval Δt is $\Phi(z)\ \Delta t$. Integrating this quantity over the entire dust column leads to a time-dependent estimate of R. This time dependence is converted to a downstream spatial dependence by the transformation $\Delta d = U\Delta t$, where U is the horizontal transport speed. We then compute M(d) is from Eq.(11). We assume U = 20m/s, consistent with Saharan dust transport.

Four initial PSDs were tested. Three are based on a simple power law:

$$\frac{dm}{d(\log r)} = Ar^{\beta} \quad , \qquad (15)$$

where A and β are constants and $r \leq 32\ \mu m$. For $\beta = 1.0$, dm/d(log r) resembles a typical Saharan source region PSD (see, for example, the upper curve in Fig.7). The submicron fraction for this distribution is 3.1 percent by mass. For comparison, we also tested two cases with the same initial mass concentration (700 $\mu g/m^3$), but a finer distribution ($\beta = 0.5$; submicron fraction = 16.3 percent) and a coarser distribution ($\beta = 1.5$; submicron fraction = 0.6 percent). These PSDs are plotted in Fig.12. A least-square fit to the PSDs observed in the Johnie Boy stabilized cloud [Nathans, Thews, and Russell, 1970] was also used as an initial condition. For $r_{max} = 32\mu m$, the Johnie Boy submicron fraction is 19 percent by mass (normalized such that the initial mass concentration is 700 $\mu g/m^3$).

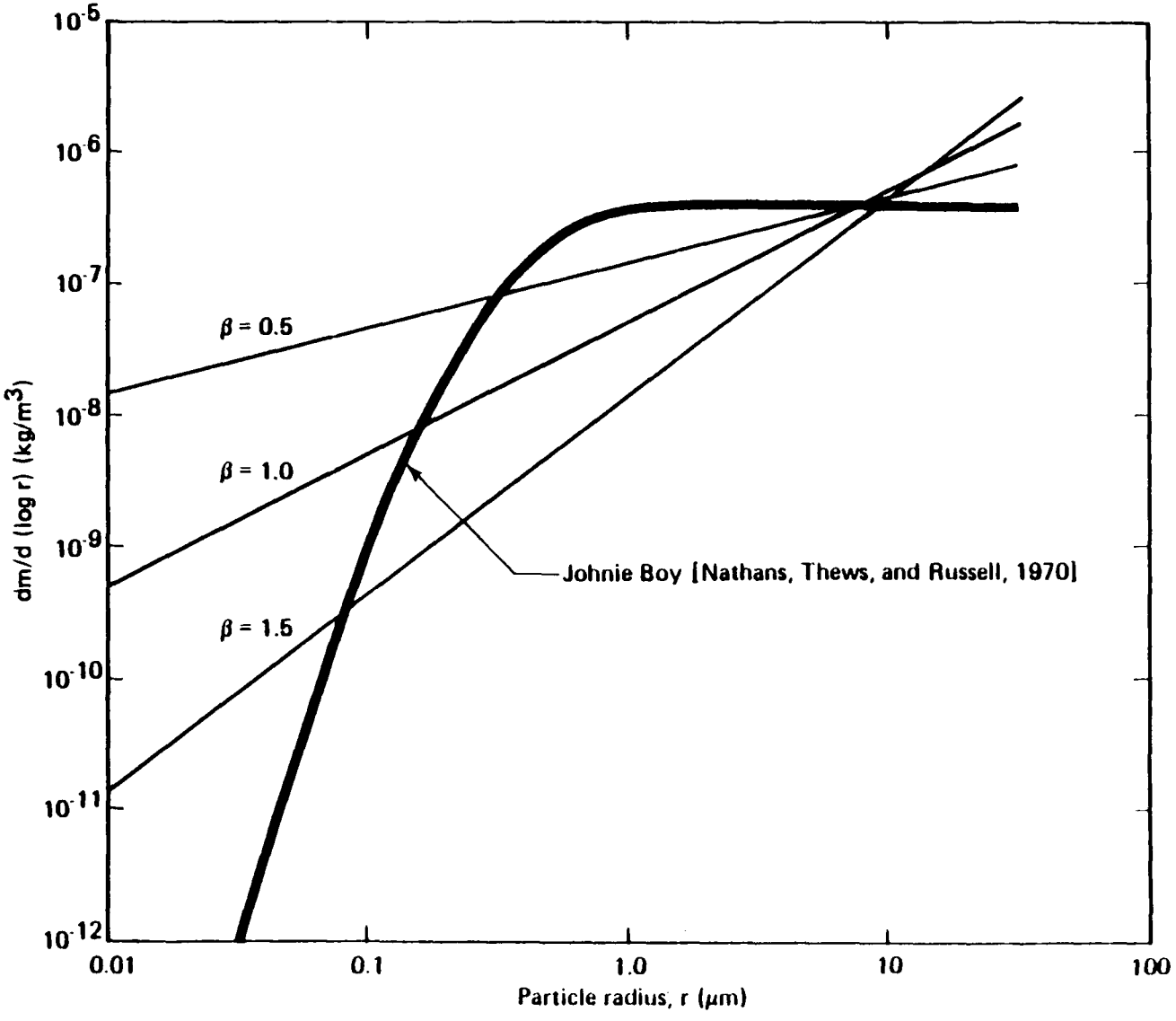

Figure 12. Three hypothetical power-law PSDs for low-altitude nuclear bursts and least-squares fit to observed subsurface burst PSD (mass concentration is 700 $\mu g/m^3$).

The normalized column density for all four cases was computed for a total transport time of five days. For U = 20 m/s, this is equivalent to d ≈ 8600 km. The results are shown in Fig.13. In all cases the exponential dependence of M on d is qualitatively similar to the Saharan case (Fig.5). However, it is clear from Fig. 13 that the Johnie Boy distribution had the greatest concentration of micron-size particles. This is evident in the rapid initial decrease in column density. The subsequent decay is much slower—almost as if the initial PSD was bimodal. Indeed, the Johnie Boy distribution was more consistent with a buried or surface burst than a near-surface air burst PSD (see, for example, Pinnick, Fernandez, and Hinds, 1983).

There is a strong dependence of the depletion rate on the initial PSD. In particular, the greater the initial concentration of large ($r > 1$ μm) particles, the greater the initial depletion rate. On the other hand, since these particles are rapidly depleted, the late-time dust cloud consists largely of submicron-size particles. Hence, for large d, M is proportional to the initial submicron fraction; at d = 8000 km, M ($\beta = 0.5$) is nearly five times larger than M($\beta = 1.5$). The change in M over most of the lifetime of a nuclear cloud subject only to dry deposition is determined primarily by the initial concentration of submicron-size particles. Larger particles have only a transient effect upon the mass deposition rate.

Late-time depletion is accelerated by coagulation and precipitation. These effects were not included in the four calculated cases. Rain—particularly over the North Atlantic—would accelerate dust removal from the troposphere. Similarly, coagulation would accelerate the sedimentation rate. Finally, Eqs. (11), (12), and (13) account for neither lateral spreading (diffusion) of the nuclear cloud nor wind shear. Nevertheless, the results demonstrate the strong sensitivity of mass removal rates to changes in the initial PSD.

RADIATIVE EFFECTS.

Saharan plumes are highly reflective at solar wavelengths, and absorption is rather weak. These characteristics are dictated by (1) the composition of the dust particles (primarily silicates), and (2) the size of the particles. Nuclear dust clouds that have a similar composition and size distribution are likely to have similar radiative properties. However, dust lofted from U.S. and Soviet silo fields would have a heavier organic content than Saharan dust, resulting in greater absorption and increased cloud optical depths. As a consequence, there may be some warming in the upper troposphere and stratosphere. This, in turn, would tend to stabilize the atmosphere and possibly suppress mid-latitude storm activity. A similar mechanism has been observed on Mars during major dust storms [Haberle, 1986].

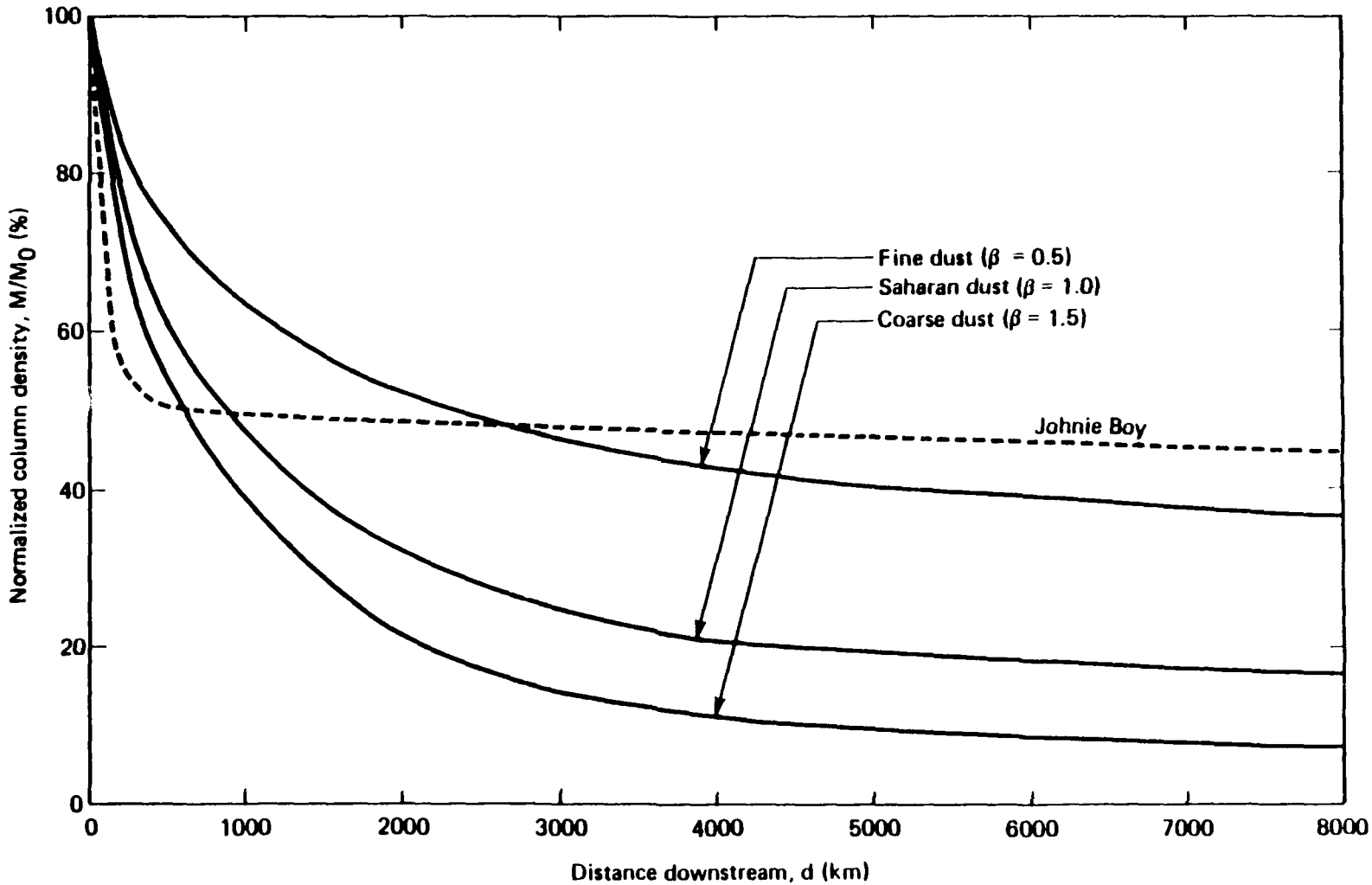

Figure 13. Computed normalized column densities as function of distance downstream for four initial PSDs.

SECTION 5

CONCLUSIONS

We find that the mass of Saharan dust lofted is comparable to about one-third the injection expected from a full-scale counterforce attack against a U.S. Minuteman missile field. The amount of dust raised is highly dependent upon soil condition and type and can vary significantly with season. Seasonal changes in vegetation, soil moisture, and the presence of surface crust reduce the scouring efficiency in Saharan source regions. Similar dependencies are expected in U.S. and Soviet silo fields where cultivation, vegetation growth cycles, ground freeze, and snow cover are factors. In the nuclear case, soils are further modified by thermal and blast effects.

Lofting of Saharan dust is qualitatively similar to nuclear sweepup. In both cases, strong surface winds are required to scour dust from the surface and a buoyant momentum source is needed to carry the dust to altitude. The strength of these mechanisms is several orders of magnitude larger in the nuclear case. Consequently, a wider spectrum of particle sizes is initially lofted and carried to greater altitudes. The largest particles are rapidly depleted: therefore, after several hours, particle-size distributions and mass concentrations in nuclear clouds are similar to those observed in Saharan plumes.

Saharan dust plumes extend 4 to 6 km in altitude. Nuclear clouds may reach the stratosphere. Despite the relatively shallow injection, Saharan dust is transported several thousand kilometers downstream. The long-range transport is aided by (1) the presence of a low-altitude stable layer which isolates the dust from turbulent surface processes, and (2) the absence of wet removal (precipitation scavenging). Mass depletion rates are initially $\sim$ 200 kg/km^2/h; this value decays rapidly downstream as the most massive particles are removed by sedimentation. After 2000 km, roughly 70 percent of the initial dust mass is depleted. At greater distances, depletion rates approach 2 kg/km^2/h: the exact value is proportional to the initial concentration of submicron-radius particles and boundary layer turbulence. Nuclear clouds, which may contain a large mass of very fine recondensed particles, would retain more of their initial mass at late times. In middle latitudes, where nuclear clouds originate, precipitation scavenging is likely to dominate the mass depletion. This scavenging is enhanced when the cloud contains large numbers of submicron-size clay ice nuclei particles. Saharan plumes thus represent an upper limit to the longevity of dust in the lower troposphere.

Far from the source, very large particles ($r > 10$ μm) are sometimes found in the Saharan plume. This may be evidence of cloud-aided coagulation. Nuclear clouds, which encounter moisture clouds more often, may contain a greater concentration of such ultragiant particles, presenting a hazard to aircraft and other flight vehicles.

Saharan dust has a very low organic content, while dust from likely target areas would have a greater organic content. Nuclear clouds are therefore more absorptive (at least at solar wavelengths) than Saharan plumes. We also find that nuclear clouds are probably less reflective than Saharan plumes due to greater concentrations of submicron-size particles. Optical depths in the more massive Saharan outbreaks may approximate those expected in nuclear clouds.

Saharan plumes provide an ideal natural analogue for the late-time removal of dust from the lower troposphere in the absence of precipitation. Removal rates as a function of downstream distance are well determined. Saharan plumes are therefore appropriate test cases for nuclear dust transport models.

SECTION 6

LIST OF REFERENCES

Bacon, D. P., T. J. Dunn, and R. A. Sarma, *Dust Producing Targets in the United States*, Science Applications International Corporation, La Jolla, California, SAIC-88/1558, 1988.

Bertrand, J., J. Baudet, and A. Drochon, "Importance des aerosols naturels en Afrique de l'Ouest," *J. Rech. Atmos.*, Vol. 8, 1974.

Brinkman, A. W., and J. McGregor, "Solar Radiation in Dense Saharan Aerosol in Northern Nigeria," *Quart. J. Roy. Meteorol. Soc.*, Vol. 109, 1983, pp. 831-847.

Carder, K. L., et al., "Dynamics and Composition of Particles from Aeolian Input Event to the Sargasso Sea," *J. Geophys. Res.*, Vol.91, 1986, pp. 1055-1066.

Carlson, T. N., "Atmospheric Turbidity in Saharan Dust Outbreaks as Determined by Analyses of Satellite Brightness Data," *Monthly Weather Rev.*, Vol. 107, 1979, pp. 322-335.

Carlson, T. N., and S. G. Benjamin, "Radiative Heating Rates for Saharan Dust," *J. Atmos. Sci.*, Vol. 37, 1980, pp 193-213.

Carlson, T. N., and R. S. Caverly, "Radiative Characteristics of Saharan Dust at Solar Wavelengths," *J. Geophys. Res.*, Vol. 82, 1977, pp. 3141-3152.

Carlson, T. N., and J. M. Prospero, "The Large-Scale Movement of Saharan Air Outbreaks over the Northern Equatorial Atlantic," *J. Appl. Meteorol.*, Vol. 11, 1972, pp. 283-297.

Delany, A. C., et al., "Airborne Dust Collected at Barbados," *Geochim. Cosmochim. Acta*, Vol. 31, 1967, pp. 885-909.

Diaz, H., et al., "A Study of the Structure and Dynamics of the Saharan Air Layer over the Equatorial Atlantic during BOMEX," *Tech. Memo. ERL WMPO-32*, National Oceanic and Atmospheric Administration, Boulder, Colorado, 1976.

Ganor, E., and Y. Mamane, "Transport of Saharan Dust across the Eastern Mediterranean," *Atmos. Environ.*, Vol. 16, 1982, pp.581-587.

Gillette, D. A., "Major Contributions of Natural Primary Continental Aerosols: Source Mechanisms," in T. J. Kneip and P. J. Lioy (eds.), *Aerosols: Anthropogenic and Natural, Sources and Transport*, New York Academy of Sciences, New York City, 1980.

Gillette, D. A., I. H. Blifford, Jr., and C. R. Fenster, "Measurements of Aerosol Size Distributions and Vertical Fluxes of Aerosols on Land Subject to Wind Erosion," *J. Appl. Meteorol.*, Vol. 11, 1972, pp.977-987.

Gillette, D. A., et al., "Threshold Velocities for Input of Soil Particles into the Air by Desert Soils," *J. Geophys. Res.*, Vol.85, 1980, pp. 5621-5630.

Gillette, D. A., et al., "Threshold Friction Velocities and Rupture Moduli for Crusted Desert Soils for the Input of Soil Particles into the Air," *J. Geophys. Res.*, Vol. 87, 1982, pp.9003-9015.

Glaccum, R. A., and J. M. Prospero, "Saharan Aerosols over the Tropical North Atlantic: Mineralogy," *Mar. Geol.*, Vol. 37, 1980, pp.295-321.

Goude-Gaussen, G., et al., "Saharan Dust on Fuertaventura Island (Canaries): Chemical and Mineralogical Characteristics, Air Mass Trajectories, and Probable Sources," *J. Geophys. Res.*, Vol.92, 1987, pp. 9753-9771.

Haberle, R. M., "Interannual Variability of Global Dust Storms on Mars," *Science*, Vol. 234, 1986, pp. 459-461.

Hartenbaum, B., *Lofting of Particulates by a High Speed Wind*, Defense Nuclear Agency, Washington, DC, DNA 2737F, 1971.

Jaenicke, R., and L. Schütz, "Comprehensive Study of Physical and Chemical Properties of the Surface Aerosols in the Cape Verde Islands Region," *J. Geophys. Res.*, Vol. 83, 1978, pp. 3583-3599.

Junge, C. E., "The Importance of Mineral Dust as an Atmospheric Constituent," in C. Morales (ed.), *Saharan Dust*, John Wiley and Sons, New York City, 1979, pp. 49-60.

Lee, I-Y, "Simulation of Transport and Removal Processes of the Saharan Dust," *J. Clim. Appl. Meteorol.*, Vol. 22, 1983, pp. 632-639.

Mason, B. J., *The Physics of Clouds*, Clarendon Press, Oxford, England, 1971.

Mirels, H., "Turbulent Boundary Layer Behind Constant Velocity Shock Including Wall Blowing Effects," *J. AIAA*, Vol. 22, 1984, pp. 1042-1047.

Nathans, M. W., R. Thews, and I. J. Russell, "The Particle Size Distribution of Nuclear Cloud Samples," in E. C. Freiling (ed.) *Radionuclides in the Environment*, American Chemical Society, Washington, DC, 1970.

National Research Council, *The Effects on the Atmosphere of a Major Nuclear Exchange*, National Academy Press, National Academy of Sciences, Washington, DC, 1985.

Patterson, E. M., and D. A. Gillette, "Commonalities in Measured Size Distributions for Aerosols Having a Soil-Derived Component," *J. Geophys. Res.*, Vol. 82, 1977, pp. 2074-2082.

Pinnick, R. G., G. Fernandez, and B. D. Hinds, "Explosion Dust Particle Size Measurements," *Appl. Optics*, Vol. 22, 1983, pp. 95-102.

Pittock, A. B., *et al.*, *Environmental Consequences of Nuclear War*, Vol. 1, *Physical and Atmospheric Effects*, John Wiley and Sons, Chichester, United Kingdom, 1986.

Prodi, F., and G. Fea, "A Case of Transport and Deposition of Saharan Dust over the Italian Peninsula and Southern Europe," *J. Geophys. Res.*, Vol. 84, 1979, pp. 6951-6960.

Prospero, J. M., and T. N. Carlson, "Vertical and Areal Distributions of Saharan Dust over the Western Equatorial North Atlantic Ocean," *J. Geophys. Res.*, Vol. 77, 1972, pp. 5255-5265.

Prospero, et al., "Dust in the Caribbean Atmosphere Traced to an African Dust Storm," *Earth Planet. Sci. Lett.*, Vol. 9, 1970, pp.287-293.

Riehl, H., *Climate and Weather in the Tropics*, Academic Press, London, 1979.

Rosenblatt, M., *Introduction to Nuclear Dust Debris Cloud Formation*, California Research and Technology, Inc., Woodland Hills, California, CRT3370, 1981 (subsequently published by Defense Nuclear Agency, Washington, DC, as Report 5832T).

Schütz, L., "Long-Range Transport of Desert Dust with Special Emphasis on the Sahara," in T. J. Kneip and P. J. Lioy (eds.), *Aerosols: Anthropogenic and Natural, Sources and Transport*, New York Academy of Sciences, New York City, 1980, pp. 515-532.

Tullet, M. T., "A Dust Fall on 6 March 1977," *Weather*, Vol. 33, 1978, pp. 48-52.

Turco, R. P., et al., "Nuclear Winter: Global Consequences of Multiple Nuclear Explosions," *Science*, Vol. 222, 1983, pp.1283-1292.

Westphal, D. L., O. B. Toon, and T. N. Carlson, "A Two-Dimensional Numerical Investigation of the Dynamics and Microphysics of Saharan Dust Storms," *J. Geophys. Res.*, Vol. 92, 1987, pp. 3027-3049.

Yoon, B. L., et al., *A Sensitivity Study for Airborne Dust and Radiation Environment Modeling*, Defense Nuclear Agency, Washington, DC, DNA-TR-85-231, 1986.

DISTRIBUTION LIST

DNA-TR-88-142

DEPARTMENT OF DEFENSE

ASSISTANT TO THE SECRETARY OF DEFENSE ATOMIC ENERGY
ATTN: EXECUTIVE ASSISTANT

DEFENSE INTELLIGENCE AGENCY
ATTN: RTS-2B

DEFENSE NUCLEAR AGENCY
3 CYS ATTN: SPWE MAJ WADE
ATTN: NASF
ATTN: OPNA
2 CYS ATTN: TITL

DEFENSE NUCLEAR AGENCY
ATTN: NVCG

DEFENSE NUCLEAR AGENCY
ATTN: TDNM
ATTN: TDTT
2 CYS ATTN: TDTT/ SUMMA

DEFENSE TECHNICAL INFORMATION CENTER
2 CYS ATTN: DTIC/ FDAB

JOINT STRAT TGT PLANNING STAFF
ATTN: JK ATTN: DNA REP
ATTN: JKCS, STUKMILLER

THE JOINT STAFF
ATTN: J-5 NUCLEAR & CHEMICAL DIV
ATTN: JAD- SFD
ATTN: JAD- SSD

DEPARTMENT OF THE ARMY

U S ARMY MATERIAL TECHNOLOGY LABORATORY
ATTN: DRXMR-HH J DIGNAM

U S ARMY NUCLEAR & CHEMICAL AGENCY
ATTN: MONA-NU

U S ARMY NUCLEAR EFFECTS LABORATORY
ATTN: ATAA-TDC R BENSON

USA SURVIVABILITY MANAGMENT OFFICE
ATTN: SLCSM-SE J BRAND

DEPARTMENT OF THE NAVY

NAVAL RESEARCH LABORATORY
ATTN: CODE 7920 A WILLIAMS

NAVAL WEAPONS EVALUATION FACILITY
ATTN: CLASSIFIED LIBRARY

OFC OF THE DEPUTY CHIEF OF NAVAL OPS
ATTN: OP 654

DEPARTMENT OF THE AIR FORCE

AERONAUTICAL SYSTEMS DIVISION
ATTN: ASD/ ENSSS H GRIFFIS

AIR FORCE TECHNICAL APPLICATIONS CTR
ATTN: TX

AIR UNIVERSITY LIBRARY
ATTN: AUL-LSE

BALLISTIC MISSILE OFFICE
ATTN: ENS
ATTN: MYE

HQ USAF/ XOXFS
ATTN: AFXOOTS

SECRETARY OF AF/ AQQS
ATTN: AF/ RDQI

STRATEGIC AIR COMMAND/ XRFS
ATTN: XRFS

WEAPONS LABORATORY
ATTN: NTES
ATTN: SUL

WRIGHT RESEARCH & DEVELOPMENT CENTER
ATTN: AFWAL/ MLBT/ J ANSPACH

DEPARTMENT OF ENERGY

LOS ALAMOS NATIONAL LABORATORY
ATTN: S S HECKER

OTHER GOVERNMENT

CENTRAL INTELLIGENCE AGENCY
ATTN: OSWR/ NED

DEPARTMENT OF DEFENSE CONTRACTORS

ACUREX CORP
ATTN: C WOLF

AEROJET GENERAL CORP
ATTN: A COLLINS

AEROSPACE CORP
ATTN: H BLAES

APPLIED & THEORETICAL MECHANICS INC
ATTN: J M CHAMPNEY

APTEK, INC
ATTN: T MEAGHER

AVCO CORPORATION
ATTN: A PALLONE
ATTN: W REINECKE

CALIFORNIA RESEARCH & TECHNOLOGY INC
ATTN: K KREYENHAGEN
ATTN: M ROSENBLATT

CALSPAN CORP
ATTN: M DUNN

CARPENTER RESEARCH CORP
ATTN: H J CARPENTER

G B LABORATORY INC
ATTN: G BURGHART

GENERAL ELECTRIC CO
ATTN: A GARBER
ATTN: B MAGUIRE

HERCULES, INC
ATTN: P MCALLISTER

KAMAN SCIENCES CORP
ATTN: L MENTE
ATTN: P RUETENIK
ATTN: N LEE

KAMAN SCIENCES CORP
ATTN: J HARPER

KAMAN SCIENCES CORPORATION
ATTN: B GAMBILL
ATTN: DASIAC

KAMAN SCIENCES CORPORATION
ATTN: DASIAC

MARTIN MARIETTA DENVER AEROSPACE
ATTN: E STRAUSS

MCDONNELL DOUGLAS CORP
ATTN: M POTTER

MCDONNELL DOUGLAS CORPORATION
ATTN: D JOHNSON
ATTN: L COHEN

MORTON THIOKOL, INC
ATTN: J HINCHMAN

PACIFIC-SIERRA RESEARCH CORP
ATTN: H BRODE, CHAIRMAN SAGE
2 CYS ATTN: R GAJ
2 CYS ATTN: R SMALL

R & D ASSOCIATES
ATTN: P RAUSCH

R & D ASSOCIATES
ATTN: J WALTON

RAND CORP
ATTN: B BENNETT

S-CUBED
ATTN: G GURTMAN

SCIENCE APPLICATIONS INTL CORP
ATTN: J STODDARD

SCIENCE APPLICATIONS INTL CORP
ATTN: J COCKAYNE
ATTN: N LAYSON

TECHNOLOGY DEVELOPMENT ASSOCIATES
ATTN: C HARRELL
ATTN: N DISPENSIERE

TITAN CORPORATION
ATTN: P C DAVENPORT

TOYON RESEARCH CORP
ATTN: J CUNNINGHAM

TRW INC
ATTN: A ZIMMERMAN

TRW SPACE & DEFENSE SYSTEMS
ATTN: W WAMPLER

TRW SPACE & DEFENSE, DEFENSE SYSTEMS
ATTN: D GLENN
ATTN: N GUILES